

RESEARCH ARTICLE

Why do ants differ in acclimatory ability? Biophysical mechanisms behind cuticular hydrocarbon acclimation across species

Lucas Baumgart^{1,2,3}, Marti Wittke¹, Svenja Morsbach⁴, Bérengère Abou³ and Florian Menzel^{1,*}

ABSTRACT

Maintaining water balance is vital for terrestrial organisms. Insects protect themselves against desiccation via cuticular hydrocarbons (CHCs). CHC layers are complex mixtures of solid and liquid hydrocarbons, with a surprisingly diverse composition across species. This variation may translate into differential phase behaviour, and hence varying waterproofing capacity. This is especially relevant when temperatures change, which requires acclimatory CHC changes to maintain waterproofing. Nevertheless, the physical consequences of CHC variation are still little understood. We studied acclimatory responses and their consequences for CHC composition, phase behaviour and drought survival in three congeneric ant species. Colony sub-groups were kept under cool, warm and fluctuating temperature regimes. *Lasius niger* and *Lasius platythorax*, both of which are rich in methyl-branched alkanes, showed largely predictable acclimatory changes of the CHC profile. In both species, warm acclimation increased drought resistance. Warm acclimation increased the proportion of solid compounds in *L. niger* but not in *L. platythorax*. In both species, the CHC layer formed a liquid matrix of constantly low viscosity, which contained highly viscous and solid parts. This phase heterogeneity may be adaptive, increasing robustness to temperature fluctuations. In *Lasius brunneus*, which is rich in unsaturated hydrocarbons, acclimatory CHC changes were less predictable, and warm acclimation did not enhance drought survival. The CHC layer was more homogeneous, but matrix viscosity changed with acclimation. We showed that ant species use different physical mechanisms to enhance waterproofing during acclimation. Hence, the ability to acclimate, and thus climatic niche breadth, may strongly depend on species-specific CHC profile.

KEY WORDS: Climate adaptation, Cuticular hydrocarbons, Ecological niche breadth, Phase behaviour, Microrheology, Drought tolerance

INTRODUCTION

All terrestrial organisms need to maintain their water balance to survive (Chown et al., 2011; Kellermann et al., 2012). Because of their high surface-to-volume ratio (Gibbs, 1998; Blomquist and Bagnères, 2010a), insects are particularly prone to desiccation. They mostly lose water via transpiration through the cuticle, which


accounts for 80% of the total water loss (Gibbs and Rajpurohit, 2010). In times of climate change with increased probability of heat and drought waves, desiccation risk will increase for many insect species, and they will need to cope with higher water stress. Insects can reduce water loss via behavioural changes, e.g. movement to a more humid place (Spicer et al., 2017). However, the main barrier against water loss is their cuticular hydrocarbon (CHC) layer. CHCs cover the body surface of virtually all insects. Beside their waterproofing function, they carry vital communication signals (Leonhardt et al., 2016), and serve other functions such as lubricating the cuticle (Cooper et al., 2008) and enhancing foot adhesion (Drechsler and Federle, 2006).

CHC profiles show an astonishing diversity across species (Kather and Martin, 2015; Sprenger and Menzel, 2020). Even sister species can have radically different profiles (Pokorny et al., 2014; Hartke et al., 2019). Despite intraspecific variation, the profiles are specific enough that species can clearly be identified based on their profile (Kather and Martin, 2012). Some of this diversity might be due to the role of CHCs as communication signals and/or mating signals, which can require complex profiles and/or lead to sexual selection (Ferveur and Cobb, 2010; Steiger and Stöckl, 2014; Leonhardt et al., 2016). However, the composition of a CHC layer also determines its waterproofing ability. Hence, species from wet habitats often possess different profiles to those from drier ones (Van Wilgenburg et al., 2011; Menzel et al., 2017). Moreover, insects have to adjust their CHC composition to current conditions, and this affects their subsequent drought survival (Toolson and Hadley, 1979; Menzel et al., 2018; Sprenger et al., 2018). So how does waterproofing work on a physical level, and how does CHC composition affect that?

Generally, the CHC layer reduces water loss by forming a passive barrier against the outward diffusion of water. The effectiveness of this barrier is dependent on its proportion of solid components (which block diffusion more effectively) and its viscosity: according to the Stokes–Einstein relation, the diffusion coefficient of molecules is inversely proportional to viscosity (Einstein, 1905); hence, water diffusion should decrease with increasing viscosity of the CHC layer. CHC layers are complex mixtures of sometimes more than 100 different hydrocarbons (Blomquist and Bagnères, 2010b). They include *n*-alkanes, methyl-branched components and unsaturated hydrocarbons with chain lengths ranging from 21 to 50 carbons (Blomquist and Bagnères, 2010a). As a result of van der Waals forces, hydrocarbons tend to aggregate. *n*-Alkanes pack most tightly, being solid at ambient temperatures (Maroncelli et al., 1982) and melting only at temperatures >40°C (Lide, 2008). In contrast, methyl groups or double bonds hinder tight packing and thus strongly reduce melting temperatures (Gibbs and Pomonis, 1995; Gibbs, 1998, 2002). As a consequence, alkenes, and at least some methyl-branched alkanes are liquid at ambient temperature. For the same chain length, the melting temperature decreases in the order *n*-alkanes, mono-methyl alkanes, di-methyl alkanes, alkenes and

¹Institute of Organismic and Molecular Evolution (iomE), Johannes Gutenberg-University Mainz, Hanns-Dieter-Hüsch-Weg 15, 55128 Mainz, Germany. ²Institute of Biology II, RWTH Aachen University, Worringerweg 2, 52074 Aachen, Germany. ³Matière et Systèmes Complexes (MSC), UMR CNRS 7057, Université de Paris, 75205 Paris Cedex 13, France. ⁴Max Planck Institute for Polymer Research, Ackermannweg 10, 55128 Mainz, Germany.

*Author for correspondence (menzelf@uni-mainz.de)

 L.B., 0000-0003-1006-0659; F.M., 0000-0002-9673-3668

alkadienes (Gibbs, 1998). In addition, the position of the methyl branch affects melting, with more terminally branched alkanes having higher melting temperatures (Gibbs and Pomonis, 1995). Melting points also increase with chain length (Gibbs and Pomonis, 1995).

Therefore, the CHC layer is not uniform, but rather a mixture of solid and liquid compounds. The phase behaviour of the CHC layer, and thus its ability to prevent evaporation, continuously changes as temperatures rise or fall – with higher temperatures, some solid CHCs may melt, and some liquid CHCs may become less viscous. As a consequence, insects adjust the CHC composition to current temperature or humidity conditions (Hadley, 1977). With increasing temperature, *n*-alkanes increase while methyl-branched alkanes decrease (Gibbs and Mousseau, 1994; Buellesbach et al., 2018; Menzel et al., 2018; Michelutti et al., 2018; Sprenger et al., 2018). However, it is still unknown how the chemical changes translate to the physical properties that determine waterproofing ability: melting range (and hence, the proportion of solid CHCs) and viscosity. For insects, an important challenge here is fluctuating temperatures, which often pose requirements entirely different from those for constant environments (Colinet et al., 2015). Here, it is crucial that a CHC layer maintains its waterproofing ability even when temperatures suddenly drop or rise. In general, however, the complexity of CHC profiles makes it difficult to predict their physical behaviour. Hence, we need to understand the physical mechanisms of waterproofing, as well as the effects of acclimatory changes, to fully appreciate how CHC composition determines the climatic niche of an insect.

In this work, we investigated acclimation and its biological, chemical and physical consequences in three species of the genus *Lasius*. *Lasius niger*, *L. platythorax* and *L. brunneus* all have different CHC profiles, and, while sympatric in Central Europe, occur in different habitats (Seifert, 2008). Our aim was to investigate species-specific acclimation responses of their CHC profile to different temperatures and their effects on drought survival at different temperatures. Using a microrheology technique that has been adapted for the study of insects (fluid quantities of the order of 100 pl) (Abou et al., 2010), as well as differential scanning calorimetry (DSC), we aimed to find links between the CHC profile, its physical properties and the ants' ability to enhance drought resistance via acclimation. Our research questions were: (1) how do acclimatory CHC changes differ between ant species?; (2) how do acclimatory changes translate to the phase behaviour of the CHC layer, i.e. how is waterproofing achieved on a physical level?; and (3) do acclimatory strategies differ between species, and how do they affect drought survival?

MATERIALS AND METHODS

Study organisms and setup of experimental colonies

We investigated three ant species: *Lasius niger* (Linnaeus 1758), *L. platythorax* (Seifert 1991) and *L. brunneus* (Latreille 1798), all of which occur in central Europe. From each species, we collected 12 colonies in the surroundings of Mainz, Germany (*L. niger*: on meadows near the University of Mainz; *L. platythorax*: from the forest floor of the Ober-Olmer forest; *L. brunneus* at tree trunks in the Gonsenheimer forest). Each colony of *L. niger* and *L. platythorax* was divided into two groups for a separate study (Wittke et al., 2022). Each of the two groups then was further split into three sub-groups. Sub-groups of group 1 ('small boxes') were kept in small plastic boxes (95×95×60 mm, Westmark GmbH, Lennestadt-Elspe, Germany) with a plastered ground and a cavity (ca. 50×30×3 mm) covered with glass plates and red foil and walls

coated with Fluon® (Whitford GmbH, Diez, Germany). Each box consisted of 20 foragers (collected outside the nest), 20 nurses (collected inside the nest, if possible, directly from the brood), at least five brood items, mostly larvae and in some cases pupae, and no queens. Group 2 sub-groups ('large boxes') were kept in three larger plastic boxes (235×175×90 mm) with a plastered ground and walls coated with Fluon®; they were kept in their original nesting material (i.e. soil for *L. niger* and soil, pieces of wood and moss for *L. platythorax*). Each group 2 box consisted at least 60 foragers (collected outside the nest), 60 nurses (collected inside the nest, if possible, directly from the brood) and at least 20 brood items, mostly larvae and in some cases pupae. Except for one box (*L. platythorax*, fluctuating temperature treatment), all group 2 boxes were queenless as well. For *Lasius brunneus*, we only had group 1 boxes, because this is an arboreal species, such that we could not collect entire colonies without destroying the nest tree. Here, we used worker groups, which were divided into three sub-groups per colony as above. Each box consisted of at least 20 foragers (collected outside the nest) and no brood items, because these could not be collected as a consequence of their arboreal nesting. All boxes were covered with lids and sealed with Parafilm™ (Bemis Flexible Packaging, Neenah, WI, USA) to ensure constant humidity. Honey, dead crickets and water in Eppendorf cups (Eppendorf AG, Hamburg, Germany) with a cotton plug were provided twice a week *ad libitum*. See Fig. 1 for a visual guide for the used methodology.

Acclimation treatments

We set up three temperature treatments: constant temperature at 20°C or 28°C and a fluctuating temperature treatment. The fluctuating temperature treatment had 20°C at night (8 h) and 28°C during the day (8 h), with 4 h ramps between the two temperatures. All treatments had a 12 h:12 h light:dark cycle. Relative humidity inside these stock colonies was kept at nearly 100% by placing water on the plaster until it was saturated. All climate treatments were maintained in climate cabinets (Rubarth Apparate GmbH, Frankfurt am Main, Germany). Climatic conditions were surveyed using data loggers (testo 174H, Testo SE & Co. KGaA, Titisee-Neustadt, Germany). From each source colony, we placed one small and (for *L. niger* and *L. platythorax*) one large sub-group in each of the three climate treatments and let the ants acclimate for 3 weeks.

Chemical analysis

After 3 weeks of acclimation, we analysed the chemical profile of the ants (total *n*=360). We used two outside workers (foragers) from each large box of *L. niger* and *L. platythorax* and from the small boxes of *L. brunneus* (*L. niger* *N*=66; *L. brunneus* *N*=54; *L. platythorax* *N*=57), as well as two nurses of each small box of *L. niger* and *L. platythorax* (*L. niger* *N*=72; *L. platythorax* *N*=67). Each worker was placed individually into a 1.5 ml glass vial (Chromatographie Zubehör Trott, Kristel, Germany) and frozen at –20°C until extraction. CHCs were extracted by immersing the ant for 10 min in *n*-hexane. We added 100 ng *n*-octadecane (solved in 10 µl *n*-heptane) as an internal standard for quantification of the absolute CHC amount. The samples were concentrated under a gentle nitrogen flow down to approximately 20 µl.

For each sample, 2 µl were injected into the gas chromatograph (7890A, Agilent Technologies, Santa Clara, CA, USA) at 250°C in splitless mode. The carrier gas used was helium at a flow rate of 1.2 ml min⁻¹ and the stationary phase was a Zebron Inferno DB5-MS capillary column (length 30 m, diameter 0.25 mm, 0.25 µm coating; Phenomenex Ltd, Aschaffenburg, Germany).

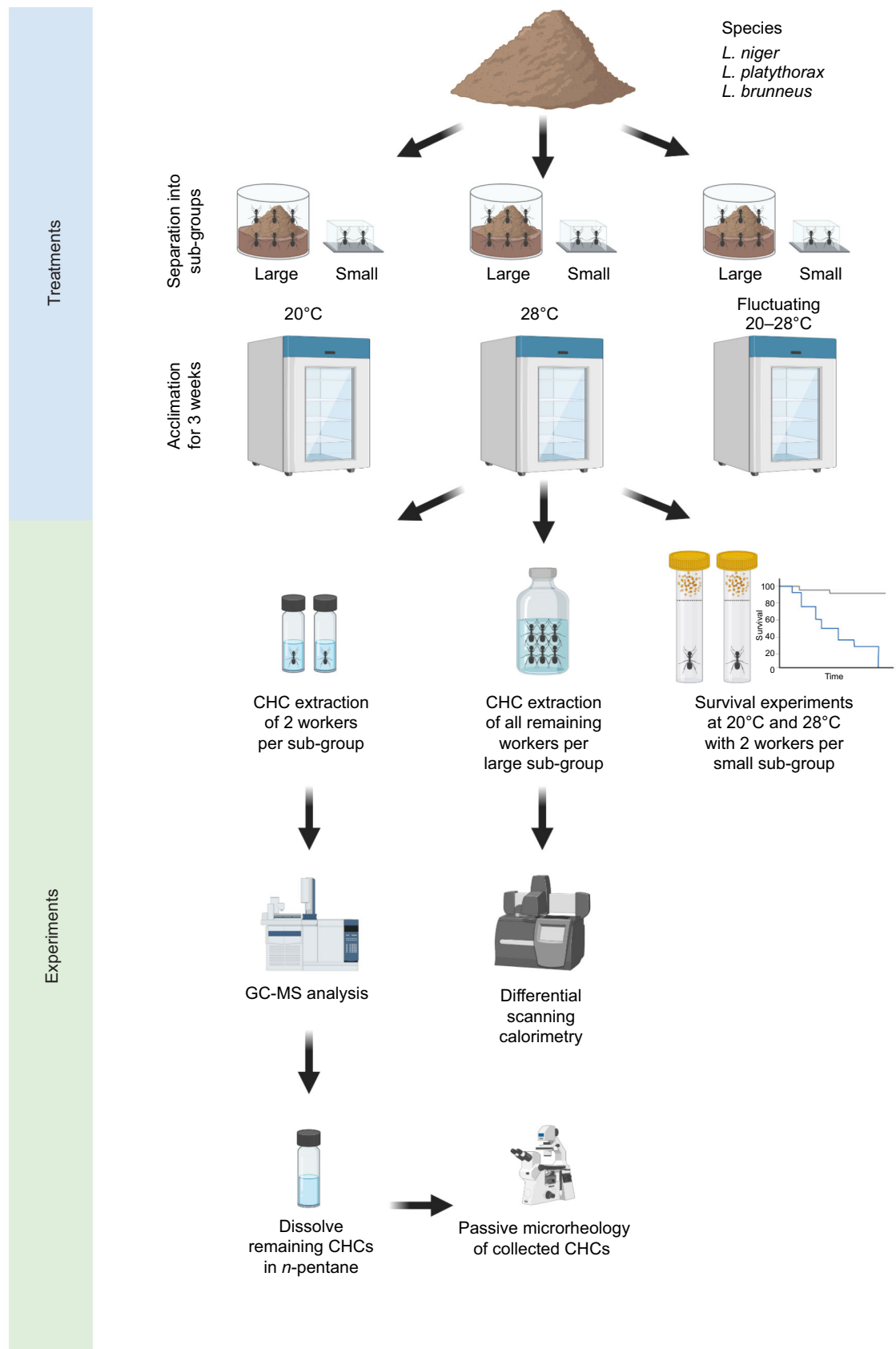


Fig. 1. Graphical overview of the experimental treatments and methods used. The division into small and large sub-groups was made because the colonies were used simultaneously for another study (Wittke et al., 2022). Note, for *L. brunneus*, only a small sub-group was used. CHC, cuticular hydrocarbon. The image was created with BioRender.com.

The temperature program started at 60°C. After 2 min, the oven heated at a rate of 60°C min⁻¹ up to 200°C and afterwards at a constant rate of 4°C min⁻¹ up to 320°C, where it was held constant for 10 min. In the mass spectrometer (5975C, Agilent Technologies), the hydrocarbons were fragmented with an ionization voltage of 70 eV. The detector scanned for molecular fragments in a range of 40–550 m z⁻¹.

We evaluated the data using the software MSD ChemStation (E.02.02. 1431, Agilent Technologies). The integration of the peaks of *L. niger* and *L. platythorax* was performed by two people (L.B. and M.W.), whereas all peaks of *L. brunneus* were integrated by L.B. only. We identified the hydrocarbons according to a retention index based on a standard series of *n*-alkanes (Carlson et al., 1998) and diagnostic ions. Non-hydrocarbon substances, hydrocarbons with a maximum (across all samples per species) below 0.5% and hydrocarbons that occurred in <20% of the samples of either species or treatment were excluded.

To test for effects of acclimation treatments, we firstly analysed univariate CHC traits, and secondly analysed the entire CHC composition. The CHC traits were the proportions of CHC classes (*n*-alkanes, mono-methyl, di-methyl and tri-methyl alkanes, alkenes, methyl alkenes and alkadienes), average chain length of *n*-alkanes and the absolute CHC quantity. For each trait and ant species, we constructed a separate linear mixed-effects model (LMM; command *lmer*, package *lme4*; <https://CRAN.R-project.org/package=lme4>) with acclimation regime (20°C, 28°C or fluctuating temperature) and sub-group type (small/large) as fixed factors (interactions allowed), and colony and (if applicable) observer as random effects. The dependent variables were transformed if necessary to obtain normally distributed model residuals (Table 1).

For the entire CHC composition, we used the proportions of all CHC classes (*n*-alkanes, mono-methyl, di-methyl and tri-methyl alkanes, alkenes, alkadienes, methyl alkenes and unknown CHCs) which added up to 1. This dataset was analysed using a PERMANOVA with the fixed factors constant/fluctuating temperature and temperature (20°C versus 28°C; nested within constant/fluctuating) and colony (R command *adonis*, package

vegan; <https://CRAN.R-project.org/package=vegan>). Interactions between the factors were allowed. Sub-group type (small versus large) was used as random factor (*strata*) except for *L. brunneus*, where there were no large sub-groups. This setup was used in order to test whether the fluctuating temperature profile differed systematically from the two constant temperature regimes, or whether it varied on the same axis as the two constant regimes. The PERMANOVA tests were done for each species separately. All statistical analyses were carried out using R v. 4.1.0 (www.r-project.org).

Differential scanning calorimetry

Melting ranges were determined using DSC. We produced separate extracts for each colony in order to obtain replicates. To obtain analysable DSC data, a high number of workers is required to extract enough sample mass. For this reason, samples for DSC could only be obtained for *L. niger* and *L. platythorax* (sample sizes *L. niger*: *N*=18 colonies; *L. platythorax*: *N*=26 colonies), as we did not have enough *L. brunneus* workers for DSC. Hexane extracts were directly transferred into DSC sample aluminium pans (100 µl volume, Mettler-Toledo GmbH, Gießen, Germany) and the solvent evaporated slowly under ambient conditions. DSC pans were covered with aluminium lids.

DSC measurements were performed on a DSC 823 instrument (Mettler-Toledo GmbH). Heating-cooling-heating cycles were recorded with a heating/cooling rate of 10 K min⁻¹ between -100 and +100°C. The measurements were performed under nitrogen atmosphere with a flow of 30 ml min⁻¹. For determination of melting ranges, the second heating cycle was evaluated to avoid effects due to sample history. Heating curves were baseline-corrected and normalized to the sample mass. For further data analysis, all melting curves for the respective acclimation treatment were then averaged and subsequently integrated in 10 K intervals between -60°C and +60°C to yield the proportionate amount of melting heat for each interval (and additionally the interval between 20 and 28°C). No significant melting was detected between -100°C and -60°C and between +60°C and +100°C. Each interval was then analysed using linear models (LM, command *lm*, package

Table 1. Statistical differences between cuticular hydrocarbon (CHC) classes from the three acclimation regimes

Class	Species	Abundance (%)	χ^2	<i>P</i>	Transformation
20°C<F<28°C					
<i>n</i> -Alkanes*	<i>L. niger</i>	7.67±0.44	56.59	<0.0001	arcsin-sqrt
Mono-methyl alkanes	<i>L. niger</i>	24.89±0.3	156.8	<0.0001	None
Mono-methyl alkanes	<i>L. platythorax</i>	14.92±0.31	228.1	<0.0001	None
Alkenes	<i>L. brunneus</i>	25.82±0.47	60.36	<0.0001	None
28°C<F<20°C					
Di-methyl alkanes	<i>L. niger</i>	55.63±0.6	97.6	<0.0001	None
Tri-methyl alkanes	<i>L. platythorax</i>	31.26±0.55	174.7	<0.0001	None
Alkenes**	<i>L. niger</i>	3.15±0.11	22.8	<0.0001	None
No treatment effects					
Di-methyl alkanes	<i>L. platythorax</i>	49.47±0.55	1.6	0.45	None
Tri-methyl alkanes	<i>L. niger</i>	5.82±0.16	3.9	0.14	sqrt
<i>n</i> -Alkanes	<i>L. platythorax</i>	2.3±0.23	15.73	0.00038	sqrt
Di-methyl alkanes	<i>L. brunneus</i>	4.42±0.11	1.5	0.47	log
Other patterns					
<i>n</i> -Alkanes***	<i>L. brunneus</i>	10.5±0.81	35.405	<0.0001	arcsin-sqrt
Mono-methyl alkanes **	<i>L. brunneus</i>	10.33±0.27	29.14	<0.0001	arcsin-sqrt
Methyl alkenes*	<i>L. brunneus</i>	12.04±0.35	61.7	<0.0001	None
Alkadienes***	<i>L. brunneus</i>	33.41±0.66	23.14	<0.0001	None

The factor 'acclimation' has 2 degrees of freedom in each model. CHC abundance is given as mean±s.e.m. for all samples of the respective ant species. See Table S4 for further statistical results. In the first two sections, all three acclimation treatments (20°C, 28°C and fluctuating temperature, F) differ from each other unless noted otherwise. *20°C and F not significantly different; **28°C and F not significantly different; ***20°C and 28°C not significantly different.

lme4) with the fixed factors species, acclimation and their interaction.

Microrheology

The phase behaviour and viscosity of CHCs from the three *Lasius* species were studied using a newly developed fluid collection procedure for insect secretion, followed by a microrheology technique adapted to small amounts of fluid of the order of 100 μl (Abou et al., 2010). For each *Lasius* species, we measured viscosity of one forager CHC extract (without internal standard) per colony and per acclimation treatment ($n=6$ colonies for *L. platythorax* and *L. brunneus*, $n=5$ colonies for *L. niger*; total $N=51$ samples).

Each CHC extract was evaporated, dissolved in 40 μl *n*-pentane for 15 min, and transferred onto a microscopic slide. After the pentane was evaporated, the CHCs were sucked up by a microsyringe with a tip of a few micrometres mounted on a three-axis piezo micromanipulator (Burleigh, Thorlabs SAS, Maisons-Laffitte, France), itself coupled to an inverted microscope (Leica DM IRB, Leica Microsystems GmbH, Wetzlar, Germany), using capillary effects. For highly viscous CHCs, we applied negative pressure to the microsyringe using the microinjector (CellTram Air, Eppendorf AG, Hamburg, Germany) for collection. Dry powder of melamine beads (diameter: 0.740 ± 0.005 μm ; Acil, Chatou, France) was deposited on a coverslip, and the collected CHCs were ejected onto the beads by applying positive pressure (Abou et al., 2010).

The motion of the tracer beads immersed in the CHC drop was recorded with a fast sCMOS camera (OrcaFlash 4.0 v2+, Hamamatsu Photonics France S.A.R.L., Massy, France) attached to the microscope with an oil immersion objective (100 \times). The camera sampled at 100 Hz at five different temperatures (30, 28, 24, 20 and 18 $^{\circ}\text{C}$) for 20 s each. Temperature was adjusted by an objective heater (Bioprotechs Inc., Butler, PA, USA), with an accuracy of $\pm 0.1^{\circ}\text{C}$. Using self-written image analysis software under ImageJ (W. S. Rasband, ImageJ, US National Institutes of Health, Bethesda, MD, USA, <https://imagej.nih.gov/ij/>, 1997–2018), the $x_i(t)$ and $y_i(t)$ positions of the beads were tracked and the mean-squared displacement (MSD) was calculated for each individual bead or averaged over several beads according to:

$$\langle \Delta r^2(t) \rangle = \langle (x_i(t' + t) - x_i(t'))^2 + (y_i(t' + t) - y_i(t'))^2 \rangle_{i,t'}. \quad (1)$$

For a purely viscous fluid, the MSD is expressed as $\langle \Delta r^2(t) \rangle = 4Dt$, giving access to the diffusion coefficient D and then to the viscosity η from the Stokes–Einstein relation $\eta = kT/6\pi R D$, where R is the bead radius, k is the Boltzmann constant and T is the temperature in Kelvin (Einstein, 1905). Most samples contained a multiphase liquid, with highly different viscosities per phase. However, the least viscous phase was by far the most abundant, as measured by the number of beads with similar viscosities. This heterogeneity of viscosities (liquid phase only) declined at higher temperatures, such that the collected samples had a homogeneous viscosity at temperatures of 28 $^{\circ}\text{C}$ or higher. Because of the heterogeneity of the collected CHCs, we conducted two different analyses: firstly, we measured the viscosity of each single bead in all samples at 24 $^{\circ}\text{C}$ for comparison; secondly, we focused on the least viscous phase in all samples, and analysed its viscosity at all measurement temperatures spanning 18–32 $^{\circ}\text{C}$.

The single-bead viscosity data were highly non-normally distributed. Therefore, we used geometric means to characterize the distribution of the single-bead viscosity data. Geometric means of all beads per sample were calculated as the exponential of the arithmetic mean of log-transformed viscosity data. In analogy,

geometric standard deviation was calculated as the exponential of the standard deviation of log-transformed data. As a measure of heterogeneity per sample, we then calculated the coefficient of variation (CV) as the variation in viscosity. The geometric means and the geometric CVs were then compared using LMM, with acclimation treatment and species as fixed factors and colony ID as random factor.

For the least-viscous phase per sample, the relationship between viscosity (as a dependent variable) and measurement temperature was first assessed using non-linear least square models (NLS). Normally distributed model residuals were only obtained after log-transformation of viscosity data. Model fits were equally good whether temperature was denoted as $1/T$ (in K^{-1}) or T (in $^{\circ}\text{C}$). Concerning Akaike's information criterion (AIC), linear dependence on measurement temperature was as good as exponential or square-root relationships (all $\Delta\text{AIC} \leq 0.067$), but significantly better than a quadratic term. Hence, we described the data using the Arrhenius law, with a linear relationship between $\log(\text{viscosity})$ and the inverse temperature ($1/T$ in K^{-1}) (De Guzmán, 1913; Eyring, 1935). In the next step, we created LMM with species, acclimation treatment and measurement temperature as explanatory variables, with all interactions allowed and colony ID as a random effect. Non-significant interactions were removed stepwise by removing the least significant interaction until AIC was minimal. All models were analysed using *Anova* (package *car*; <https://CRAN.R-project.org/package=car>).

Drought survival

We measured drought survival at two different temperatures (20 $^{\circ}\text{C}$ and 28 $^{\circ}\text{C}$, henceforth termed 'test temperatures') for each species and acclimation treatment. To this end, we used foragers from each large box (small box for *L. brunneus*). Two foragers were used per species, colony, acclimation treatment and test temperature, resulting in 432 replicates. Foragers were placed individually into a polystyrene vial (diameter 28 mm, height 64 mm, volume 30 ml, K-KTK e.K., Retzstadt, Germany). The vial was plugged with a piece of foam (12.05 ± 0.94 mm) to approximately one-third of its height, filled with silica gel (2–5 mm, i.e. 7.98 ± 0.32 g, Sigma-Aldrich Laborchemikalien GmbH, Seelze, Germany) and sealed airtight with ParafilmTM. Then, vials were placed into climate cabinets at 20 $^{\circ}\text{C}$ or 28 $^{\circ}\text{C}$.

We checked survival first after 6 h for the 20 $^{\circ}\text{C}$ experiment series (after 4 h for *L. brunneus*), after 4 h for the 28 $^{\circ}\text{C}$ experiment series and afterwards once every hour until the 24th hour of the experiment. The death of an ant was defined here as the lack of any movement even after shaking the vial. All observations were conducted blindly.

As a control group we put two foragers of three colonies from each of the large boxes of *L. niger* and *L. platythorax* (*L. niger* $N=45$; *L. platythorax* $N=48$) with a piece of a wet paper towel individually into a polystyrene vial, plugged it with a piece of foam and sealed it with ParafilmTM to exclude death caused by isolation. In the control group, where we tested whether the ants die from isolation rather than from drought stress, only three ants out of 90 died within the 24 h of the experiment.

The data were analysed with a Cox mixed-effects model (command *coxme*, R package *coxme*; <https://CRAN.R-project.org/package=coxme>) with species, acclimation temperature and experiment temperature as explanatory variables and colony ID and test day as random effects. The results for this model were too complex, which is why we created two different, more specific models. First, we created a test temperature-specific model with a

subset of the data, which only contained test temperature 20°C or 28°C, with acclimation temperature and species as explanatory and colony ID and test day as random effects. Afterwards, we checked effects species-wise for each test temperature. Second, we created a treatment-specific model with a subset of the data, which only contained the corresponding acclimation temperatures (20°C, 28°C and fluctuating) with test temperature and species as explanatory and colony ID and test day as random effects. Afterwards, we checked effects test temperature-wise for each species. Only a few ants had died before the first observation, i.e. in the first 6 h (*L. niger* $N=6$; *L. platythorax* $N=1$; *L. brunneus* $N=23$) or 4 h (*L. niger* $N=12$, *L. platythorax* $N=1$; *L. brunneus* $N=34$). As their time of death was uncertain, we conducted two parallel analyses, treating them as if they had died (a) in the first hour of the experiment or (b) directly before the first observation. The two analyses yielded comparable results, and we focus on analysis (a) in Results, but report analysis (b) in Table S3. We tested variables with type-II ANOVA (command *Anova*, package *car*; <https://CRAN.R-project.org/package=car>). Pairwise comparisons were done using a Tukey *post hoc* comparison (command *glht*, package *multcomp*; <https://CRAN.R-project.org/package=multcomp>).

RESULTS

Chemical analysis: overall CHC composition

All three species had very different CHC profiles (Fig. 2; Tables S1–S3). *Lasius niger* and *L. platythorax* both were dominated by mono-methyl, di-methyl and tri-methyl alkanes. In *L. platythorax*, all mono-methyl alkanes were internally branched. In *L. niger*, 6.2±0.19% (mean±s.e.m.) out of 24.9±0.30% were terminally branched (methyl branch positions 2–5). For *L. brunneus*, terminally branched mono-methyl alkanes represented 3.72±0.21% out of 10.3±0.27% mono-methyl alkanes. However, compared with that of *L. niger*, the profile of *L. platythorax* had higher chain lengths, more tri-methyl alkanes and fewer mono-methyl alkanes. The profile of the third species, *L. brunneus*, differed strongly from that of the others. It was dominated by alkenes, methyl alkenes and alkadienes but had only a few di- or tri-methyl alkanes.

Chemical analysis: acclimatory changes of CHC classes, chain lengths and absolute quantity

All three species showed strong, and often parallel, responses to the acclimation regimes. Some CHC classes showed lowest abundance in the 20°C treatment, highest abundance at 28°C and intermediate abundance in the fluctuating temperature treatment (Fig. 3), which would be expected for CHCs that are comparatively viscous or solid, and thus effective for waterproofing. This was true for *n*-alkanes and mono-methyl alkanes in both *L. niger* and *L. platythorax*, and for alkenes in *L. brunneus* (Table 1). Other classes were most abundant at 20°C, least abundant at 28°C and intermediate in the fluctuating temperature treatment, which would be expected for the less viscous CHCs. This was true for di-methyl alkanes in *L. niger* and tri-methyl alkanes in *L. platythorax*, and, although not all three treatments differed significantly from each other, for alkenes in *L. niger* and methyl-branched alkenes in *L. brunneus* (Table 1). Abundance did not differ among treatments for tri-methyl alkanes in *L. niger* and di-methyl alkanes in *L. platythorax* and *L. brunneus*. These CHC classes had an abundance of <7%, with the notable exception of di-methyl alkanes in *L. platythorax*, which made up around 50% of the profile. In three cases, sub-group type affected CHC class abundance: *n*-alkanes (more in small sub-groups) in *L. platythorax*, and tri-methyl alkanes

in *L. niger* and *L. platythorax* (less in small sub-groups in both species; Table S4). Interactions between acclimation treatment and sub-group type were never significant.

Only in *L. brunneus* did we find further acclimation effects that deviated from those described above (Table 1). In this species, *n*-alkanes were lowest in the fluctuating temperature treatment but similarly high in the 20°C and 28°C regimes. The opposite was found for alkadienes, which were highest for the fluctuating temperature regime, and did not differ between the 20°C and 28°C regimes. Proportions of mono-methyl alkanes in *L. brunneus* were highest in the 20°C treatment but at a similarly lower level for the 28°C and fluctuating temperature treatment. Furthermore, average chain length of *n*-alkanes in *L. brunneus* was much higher in the 28°C and fluctuating temperature treatment than in the 20°C treatment ($\chi^2=54.45$, $P<0.001$) (Fig. S1). In contrast, it did not differ among acclimation treatments in *L. niger* or *L. platythorax* (both $\chi^2<1.3$, $P>0.5$). Finally, in *L. brunneus*, all three acclimation treatments led to different absolute CHC quantities, with highest quantities in fluctuating temperature conditions, intermediate at 28°C and lowest at 20°C ($\chi^2=22.81$, $P<0.001$) (Fig. S1). In contrast, absolute CHC quantities were at most slightly affected by acclimation in *L. niger* and *L. platythorax*. In *L. niger*, CHC quantities were slightly higher for 20°C-acclimated ants (albeit not in pairwise comparisons; $\chi^2=7.58$, $P=0.02$), while there was no effect in *L. platythorax* ($\chi^2=1.92$, $P=0.38$).

The deviant patterns of *L. brunneus* were also reflected in the overall CHC composition. Acclimation treatments affected the overall CHC composition in all three species but only in *L. brunneus* did the CHC composition in fluctuating temperature conditions systematically differ from that in constant ones (PERMANOVA: pseudo- $F_1=23.3$, $P=0.001$; Table S5). This factor was not significant for *L. niger* and *L. platythorax*, where the CHC composition in the fluctuating temperature treatment was intermediate between that in the constant 20°C and constant 28°C treatments (pseudo- $F_1=0.80$, $P=0.48$ for *L. niger*; pseudo- $F_1=1.3$, $P=0.28$ for *L. platythorax*). The two constant regimes (20°C and 28°C) differed from each other in all three ant species. See Table S5 for further details.

Overall, we found that in *L. niger* and *L. platythorax*, warm acclimation led to a higher abundance of rather solid or viscous CHC classes, and a lower abundance of less viscous CHC classes. The fluctuating temperature treatment showed values in between those of the constant cool and the constant warm treatment. Hence, acclimatory changes in these two species were quite predictable overall. In *L. brunneus*, in contrast, acclimatory changes were not in line with expectations, with several counter-intuitive changes. Most notably, the fluctuating temperature treatment resulted in CHC changes that systematically differed from those in the two constant ones rather than being intermediate.

Biophysical analysis: melting behaviour

In both ant species, CHCs started to melt around –40°C, and the last CHCs liquefied at 45–50°C (Fig. 4). The largest melting peaks were observed between –25°C and –5°C, where 52.1±3.0% (*L. niger*) and 57.5±2.4% (*L. platythorax*) of all CHCs became liquid. Overall, melting ranges of *L. niger* and *L. platythorax* were surprisingly similar (Fig. 4). In particular, the 20°C-acclimated individuals of both species were hardly different, whereas differences were more pronounced for ants from the 28°C regimes. Interestingly, <7% of the CHCs melted between 20°C and 28°C, i.e. between the two acclimation temperatures. Acclimation did not affect this proportion (LM: $F_2=0.77$, $P=0.47$). In this interval, slightly more CHCs melted

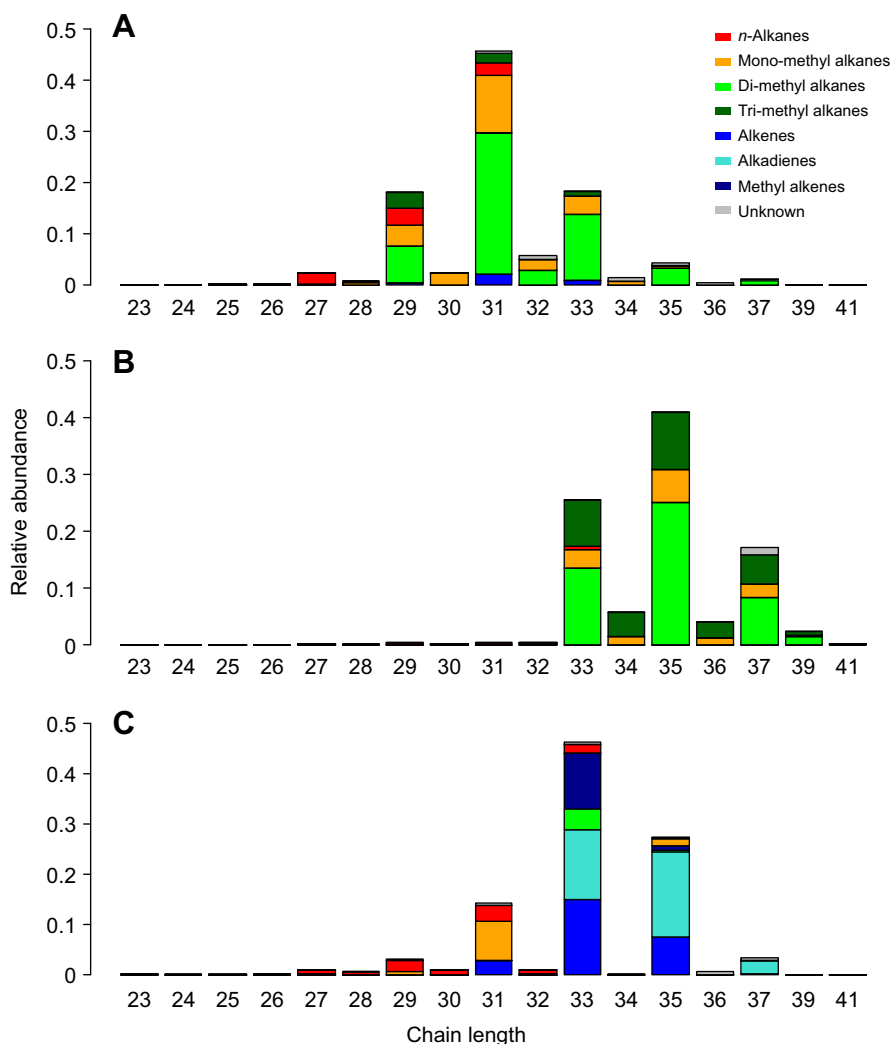


Fig. 2. Visualization of the CHC profiles of the three ant species. Relative abundance of CHCs in (A) *Lasius niger*, (B) *Lasius platythorax* and (C) *Lasius brunneus*. The x-axis denotes chain length of the CHCs; the bars represent the relative abundance of each CHC class per chain length and add up to 1.

in *L. niger* than in *L. platythorax* (LM: $F_1=4.80$, $P=0.035$; species \times acclimation: $F_2=0.14$, $P=0.87$). Generally, around 90% or more of CHCs melted below 28°C. This proportion was only lower for warm-acclimated *L. niger*. In this species, ants from the 28°C treatment had a percentage of CHCs melting below 28°C compared with the other two treatments (both $t>2.9$, $P<0.006$), whereas acclimation treatments did not differ in *L. platythorax* (LM: species: $F_1=5.7$, $P=0.022$; acclimation: $F_2=2.1$, $P=0.14$; interaction: $F_2=4.6$, $P=0.017$) (Fig. 5).

To further analyse melting ranges, we divided them into 10 K intervals. Here, strong acclimatory effects were found for the 30–40°C interval, where the proportion of melting CHCs was significantly higher for warm-acclimated ants, but only in *L. niger* (acclimation: $F_2=4.8$, $P=0.014$; species: $F_1=11.2$, $P=0.0018$; interaction: $F_2=5.3$, $P=0.0094$) (Fig. 5). A similar but weaker pattern was found for the 40–50°C interval (acclimation: $F_2=2.2$, $P=0.13$; species: $F_1=1.99$, $P=0.17$; interaction: $F_2=3.2$, $P=0.050$). In turn, a slightly lower percentage of CHCs melted in the –10°C to 0°C interval in warm-acclimated *L. niger* compared with the other climate regimes or with *L. platythorax* (acclimation: $F_2=2.6$, $P=0.091$; species: $F_1=3.4$, $P=0.075$; interaction: $F_2=0.78$, $P=0.46$). Furthermore, warm-acclimated ants of both species had significantly more CHCs melting between 10 and 20°C (acclimation: $F_2=7.3$, $P=0.0020$; species: $F_1=1.3$, $P=0.25$; interaction: $F_2=1.1$, $P=0.35$). No other effects were found for any 10 K interval.

Overall, the melting profiles of *L. niger* and *L. platythorax* were remarkably similar (*L. brunneus* could not be analysed because of the high number of workers necessary for DSC). Interestingly, only a few CHCs melted between 20 and 28°C, and this amount was independent of acclimation treatment. Thus, irrespective of acclimation treatment, the proportion of solid CHCs at 20°C was not much higher than that at 28°C. Acclimation effects were most notable in *L. niger*, where warm-acclimated ants had more CHCs melting between 30 and 50°C, and fewer CHCs melting at temperatures below 20°C. In *L. platythorax*, in contrast, acclimation affected CHC melting much less, and especially above 30°C no effect of acclimation was detectable.

Biophysical analysis: phase behaviour

All CHC extracts were highly heterogeneous, with solid and liquid phases co-occurring even at 32°C. However, even within the liquid phase, the samples developed a more heterogeneous phase behaviour with decreasing temperature, including signs of gelification (albeit less so in *L. brunneus*). This was reversible, i.e. all gelified parts liquefied when temperature was increased again. Heterogeneity was evidenced by closely spaced beads of different viscosities in the liquid phase of the same sample (Fig. S2). Across all species, the lowest viscosity level was most abundant, representing 77% of the beads (0.35 ± 0.06 mPa s, $n=246$ out of 319 beads) (Fig. 6). Therefore, viscosity was analysed firstly for all

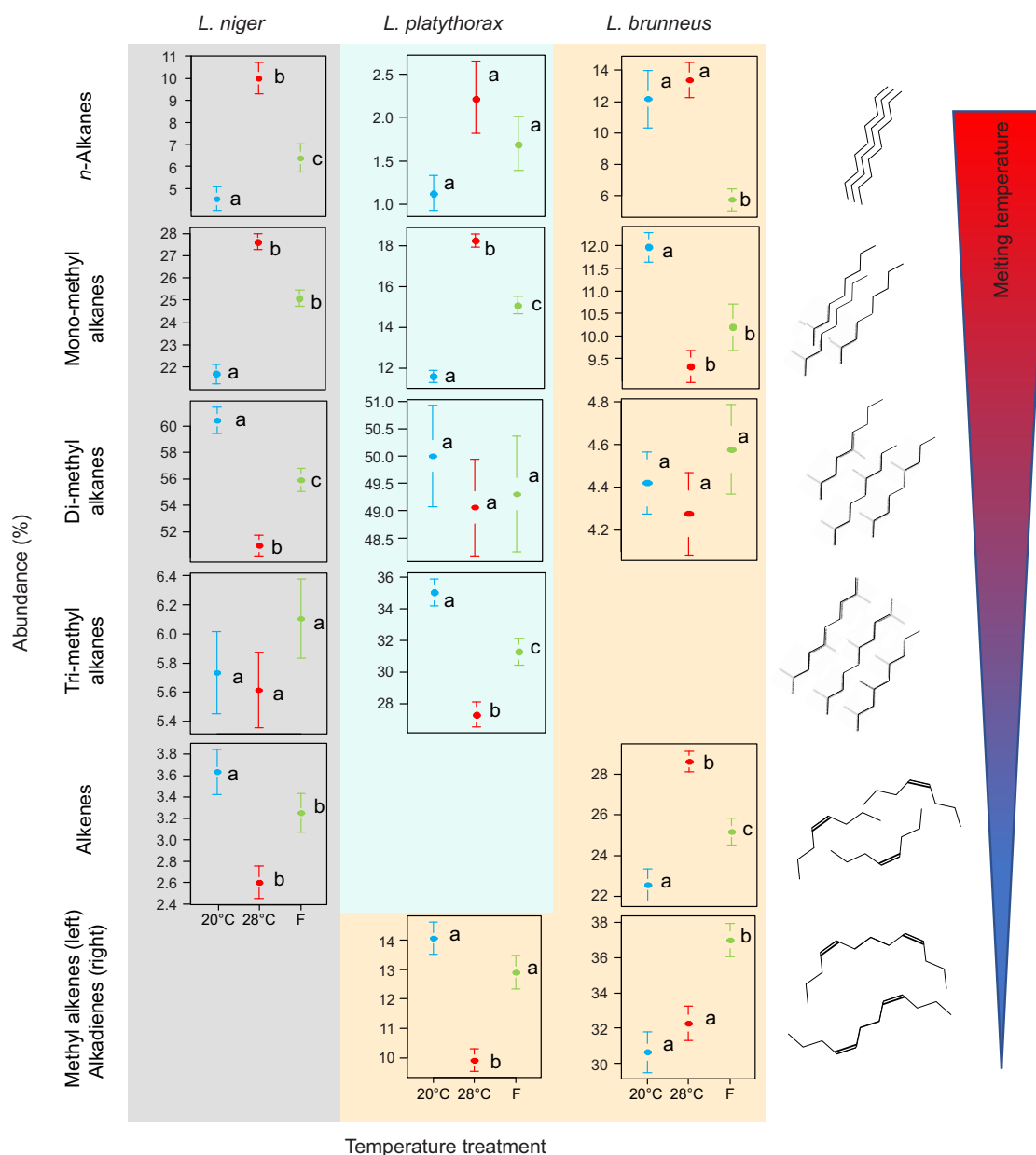


Fig. 3. Acclimatory differences in the relative abundance of each CHC class. CHC classes are sorted in order of decreasing melting temperature, from top to bottom. To the right of each row is a representation of the characteristics of each substance class. The graphs show the percentage abundance (mean \pm s.e.m.) of each CHC class for the three acclimation treatments: 20°C (blue), 28°C (red) and fluctuating temperature (F; green). The bottom row contains graphs of two CHC classes that only occurred in *L. brunneus*, i.e. methyl-branched alkenes and alkadienes. Different letters indicate a significant difference between values according to linear mixed-effects models.

viscosity levels (but only at a measurement temperature of 24°C) and secondly only for the most abundant, least viscous level (but all measurement temperatures). When including all beads, the (geometric) mean viscosity did not differ either between species or between acclimation treatments (LMM, log-transformed data: both $\chi^2_2 \leq 2.7$, $P > 0.25$; interaction: $\chi^2_4 = 6.5$, $P = 0.16$) (Fig. 7A). However, the heterogeneity in viscosity (quantified as the coefficient of variation, CV) differed between species: it was significantly lower in *L. brunneus* (LMM, square-root transformed data: $\chi^2_2 = 10.3$, $P = 0.0058$), indicating that CHC layers of *L. brunneus* are more homogeneous. Heterogeneity also differed among acclimation treatments, being higher for the fluctuating temperature treatment ($\chi^2_2 = 8.1$, $P = 0.017$). The interaction species \times acclimation was not significant ($\chi^2_4 = 4.3$, $P = 0.37$)

(Fig. 7B). Our second analysis considered only the least viscous phase (77% of all beads). Here, we analysed the effect of measurement temperature, species and acclimation treatment in a parametric Arrhenius model. As expected, measurement temperature had the highest impact on viscosity (LMM: $\chi^2 = 103.5$, $P < 0.0001$). This effect was independent of acclimation and species, i.e. none of the samples was more or less sensitive to measurement temperature (no significant interactions with measurement temperature). Interestingly, acclimation only affected viscosity of the least viscous phase in *L. brunneus* (acclimation: $\chi^2 = 34.03$, $P < 0.001$; species: $\chi^2 = 16.28$, $P < 0.001$; interaction: $\chi^2 = 65.39$, $P < 0.001$). In this species, viscosity differed between all three acclimation treatments, being highest for the 20°C treatment, intermediate for 28°C, and lowest for the fluctuating temperature

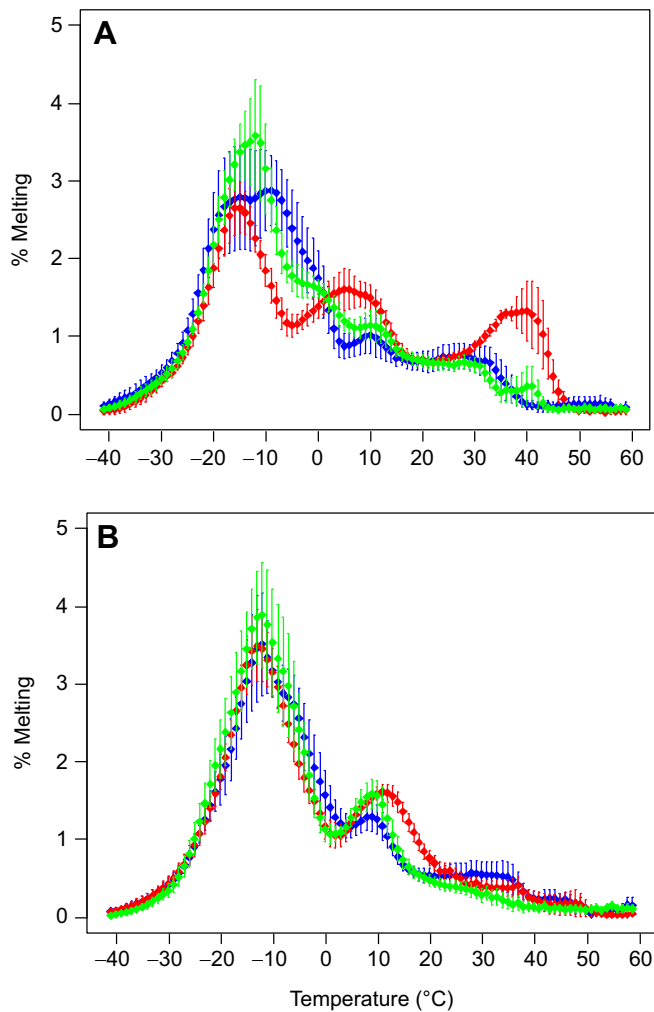


Fig. 4. Melting ranges of CHC layers. (A) *Lasius niger* and (B) *L. platythorax*. The plots show the mean (\pm s.e.m.) proportion of the CHC layer that melted in each 1 K interval, separately for 20°C acclimation (blue), 28°C acclimation (red) and fluctuating temperature acclimation (green).

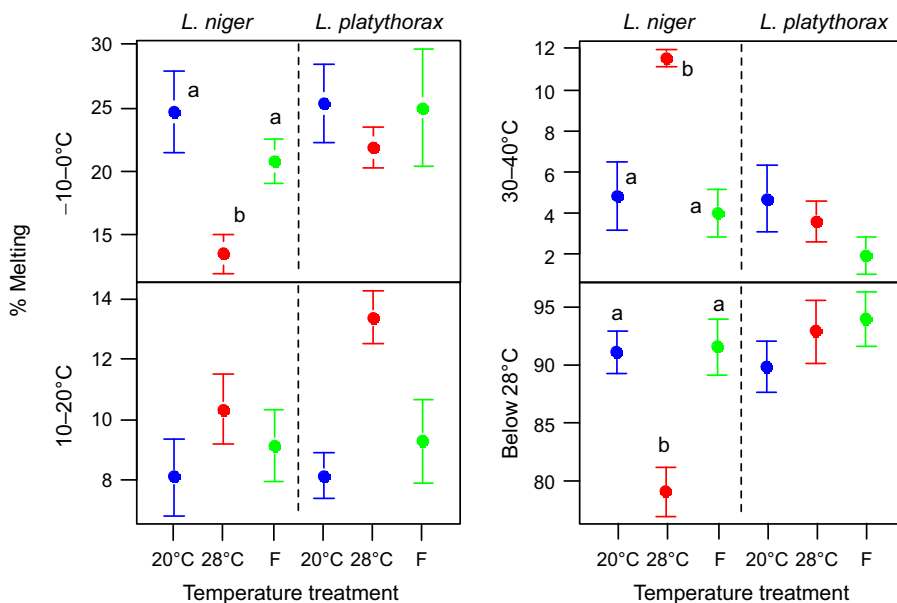


Fig. 5. Melting of CHCs in particular temperature intervals. The plots show the mean (\pm s.e.) proportion of the CHC layer in *Lasius niger* and *L. platythorax* that melted in the temperature intervals $-10-0^{\circ}\text{C}$, $10-20^{\circ}\text{C}$ and $30-40^{\circ}\text{C}$, and below 28°C , for the three acclimation treatments: 20°C (blue), 28°C (red) and fluctuating (F; green). Different letters indicate a significant difference between values according to linear models. For the $10-20^{\circ}\text{C}$ interval, significantly more CHCs melted in 28°C -acclimated ants than in both the other treatments. This was true for both species pooled but not if the species were analysed separately.

treatment (Fig. 7C). For *L. niger* and *L. platythorax*, acclimation did not change viscosity, and their values were similar to those for the fluctuating temperature treatment of *L. brunneus*.

Overall, the liquid phase of the CHCs was very heterogeneous, with patches of highly variable viscosity. While the average viscosity did not differ between species or between acclimation treatments, CHCs of *L. niger* and *L. platythorax* were more heterogeneous compared with the more homogenous *L. brunneus*. Heterogeneity was also increased in fluctuating temperature-acclimated ants. We then focused on the least viscous phase, which made up 77% of all beads. This phase behaved as predicted by Arrhenius' law in terms of the relationship between viscosity and temperature. Interestingly, acclimation effects were only detected in *L. brunneus*, where viscosity was highest for 20°C -acclimated ants, and lowest for fluctuating temperature-acclimated ants. In the other two species, viscosity of the least viscous phase did not differ among acclimation treatments.

Drought survival

Drought survival differed strongly among test temperatures, species and acclimation treatments. The highest impact was test temperature – workers dried out faster at 28°C (comprehensive Cox LME model, $\chi^2=138.24$, $P<0.001$) (Fig. 8). In general, *L. platythorax* survived longer than the other two species, but these differences were not always significant. Because of the complex statistical interactions, we constructed separate models for the two test temperatures.

Under cooler conditions, acclimation and species identity affected survival much less. At 20°C test temperature, *L. platythorax* always survived longer than the other two species (species $\chi^2=42.55$, $P<0.0001$). This difference was highest for 28°C -acclimated ants; in the fluctuating temperature treatment, *L. platythorax* survival did not significantly differ from that of *L. niger* (acclimation: $\chi^2=4.88$, $P=0.087$; species \times acclimation: $\chi^2=11.5$, $P=0.021$; Table S6).

Under warmer conditions (28°C test temperature), *L. niger* and *L. platythorax* ants were more drought resistant after warm acclimation, but this was not true for *L. brunneus* (acclimation $\chi^2=17.8$, $P<0.0001$; species $\chi^2=22.0$, $P<0.0001$; interaction $\chi^2=10.3$, $P=0.036$). In both species, acclimation to 28°C significantly enhanced survival compared with 20°C acclimation.

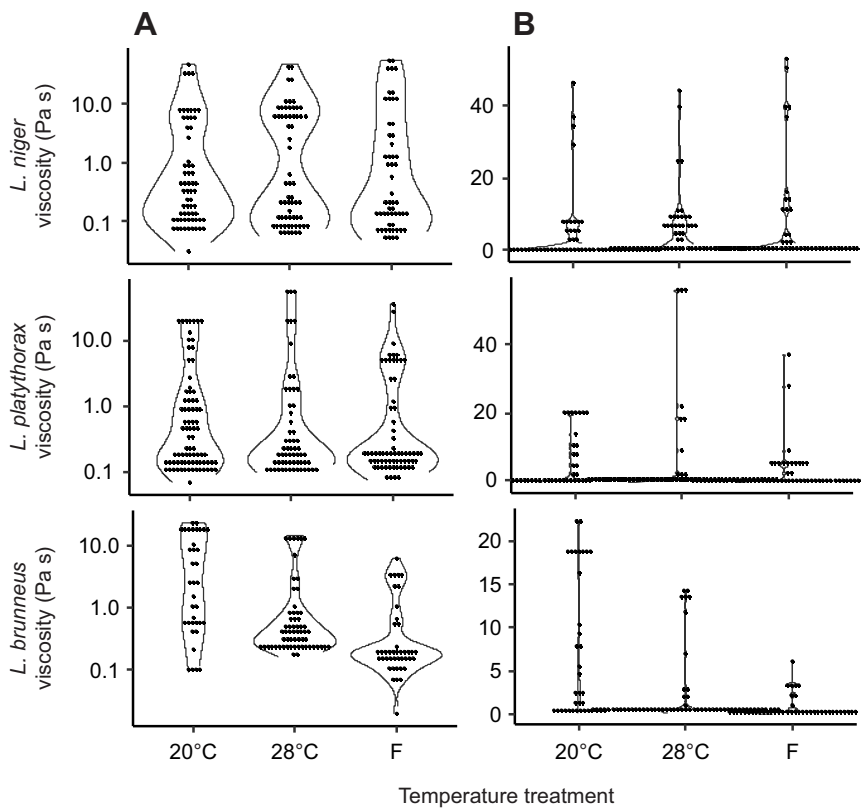


Fig. 6. Heterogeneity of CHC viscosity. The violin plots show viscosity per tracer bead (measured at 24°C) on (A) a log scale and (B) a Cartesian scale, pooled for all samples of a species and acclimation treatment (20°C, 28°C or fluctuating temperature conditions).

In *L. platythorax*, fluctuating temperature acclimation resulted in a similar survival benefit, which was less pronounced in *L. niger*. To sum up, warm acclimation increased drought survival at 28°C test temperature for *L. niger* and *L. platythorax* and at 20°C for *L. platythorax*, but not for the other treatments (Table S6, Fig. S3). In all treatments and test temperatures, *L. platythorax* survived the longest, although not always significantly longer than both of the other species. For *L. brunneus*, however, acclimation did not affect survival at all.

Overall, warm acclimation increased drought resistance, even at cooler temperatures. The acclimatory ‘gain’ in drought resistance was highest in *L. platythorax*, followed by *L. niger*. Only in *L. brunneus* did acclimation not affect survival at all.

DISCUSSION

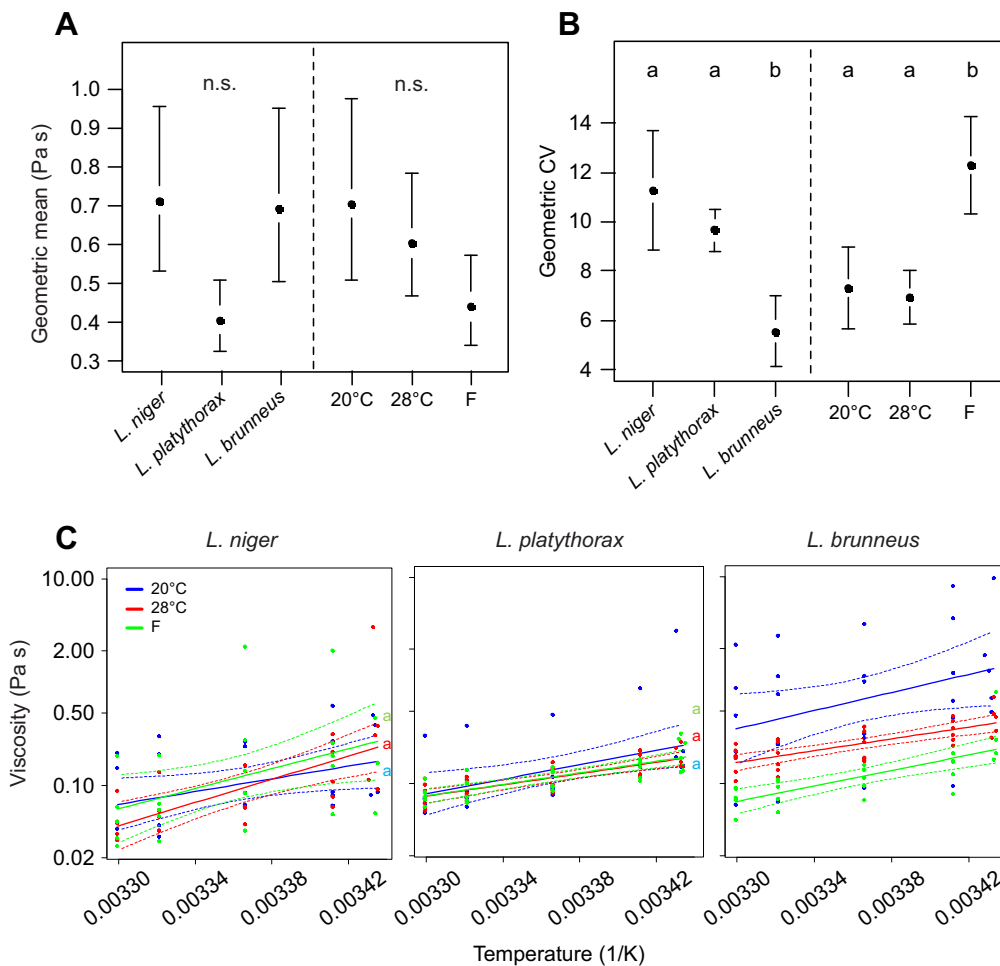
Chemical composition: which changes match predictions and which do not?

Water loss is temperature dependent. This is because at high temperatures, more CHCs melt, and the viscosity of liquid CHCs decreases. At the same time, water vapor pressure increases. All these factors increase water loss, i.e. the diffusion of water molecules, through the cuticle. To counteract this, warm-acclimated insects increase the proportion of solid or highly viscous hydrocarbons (such as *n*-alkanes or mono-methyl alkanes) at the expense of low-viscosity, low melting temperature hydrocarbons (such as alkadienes, di-methyl or tri-methyl alkanes) (Gibbs and Pomonis, 1995; Gibbs, 1998; Gibbs, 2002; Gibbs and Rajpurohit, 2010). Such patterns have been shown in the past (Hadley, 1977; Toolson and Hadley, 1979; Gibbs and Mousseau, 1994; Rajpurohit et al., 2017; Sprenger et al., 2018). Alternatively, or additionally, they might increase the CHC chain length, which also raises the melting point (Gibbs and Pomonis, 1995), and/or increase the overall CHC quantity, which reduces

water diffusion through the CHC layer without changing phase behaviour. This is why in this study, we compared acclimation strategies across species, and studied their physical mechanisms as well as their actual impacts on drought resistance. Across insects, CHC profiles are usually rich either in methyl-branched alkanes (especially di-methyl and tri-methyl alkanes) or in unsaturated hydrocarbons, but rarely both (Menzel et al., 2017; F.M., unpublished data). This is why we chose *L. niger* and *L. platythorax*, which are dominated by di-methyl or tri-methyl alkanes, and *L. brunneus*, which is dominated by unsaturated hydrocarbons.

In our study, CHC changes of *L. niger* and *L. platythorax* largely confirmed the above predictions: warm-acclimated individuals had more high melting temperature CHCs such as *n*-alkanes and mono-methyl alkanes, but fewer low melting temperature CHCs such as di- or tri-methyl alkanes. For rarer CHC classes (abundance <10%), this was not always found, however, possibly as a result of the relatively higher noise at low abundance. Nonetheless, it is surprising that the di-methyl alkanes did not change in abundance in *L. platythorax* although they contributed 50% of the profile. Interestingly, absolute CHC quantities were not part of the acclimation strategy in these species, being unaffected by acclimation or even lower in warm-acclimated species.

For *L. brunneus*, however, only some acclimatory changes are in line with the predictions – others are not. Here, alkenes increased with warm acclimation, whereas methyl alkenes decreased. This makes sense if we consider that among unsaturated hydrocarbons, unbranched alkenes are those with the highest melting point, presumably much higher than that of methyl alkenes. However, the finding that neither *n*-alkanes nor mono-methyl alkanes were upregulated in warm-acclimated ants is unexpected, even if the *n*-alkanes increased in chain length. These two classes should provide the best waterproofing, and thus the best option to improve

**Fig. 7. Viscosity of CHC layers.**

(A) Geometric mean of the viscosity (mean±s.e.) of all measured beads per sample, separated by species (left) and acclimation treatment (20°C, 28°C or fluctuating temperature conditions; right). (B) Geometric coefficient of variation (mean±s.e.) for viscosity of all measured beads per sample, shown depending on species (left) and acclimation treatment (right). (C) Viscosity of the phase with the lowest viscosity ('matrix') according to species, acclimation treatment and measurement temperature. The graphs show Arrhenius plots of log-transformed viscosity plotted against inverse temperature, with regression lines and 95% confidence intervals based on linear models. Different letters indicate a significant difference.

waterproofing. Instead, *L. brunneus* showed higher absolute CHC quantities in the warm and especially the fluctuating temperature treatment, which may be another (albeit here ineffective) way to reduce water loss.

Effect of temperature fluctuation

In *L. niger* and *L. platythorax*, workers from fluctuating treatments showed a CHC composition that was in between that of the 20°C and the 28°C treatment, which makes sense given that the average temperature of the fluctuating temperature was around 24°C. In contrast, *L. brunneus* showed very different, unexpected CHC changes when acclimating to fluctuating temperature conditions, suggesting that in this species, fluctuating conditions posed acclimatory demands that systematically differed from those of any constant regime. The fluctuating temperature regime resulted in fewer *n*-alkanes, more alkadienes, and a lower viscosity; all these effects should actually reduce desiccation resistance. Only absolute CHC quantities were highest. As a consequence, fluctuating conditions might be more costly for *L. brunneus* than for the other species: most of the observed chemical changes should rather reduce than increase waterproofing, and upregulated CHC production might be an additional metabolic cost. This tentatively suggests that for *L. brunneus*, fluctuating temperature conditions might be harder to cope with than for the other two ant species.

Heterogeneous phase behaviour may be adaptive

All CHC profiles of the three study species, regardless of acclimation treatment, were biphasic, with liquid and solid parts at

ambient temperature. Upon decreasing temperature, we often observed gelification (i.e. solidification) in some parts of the liquid phase. However, our most notable result was that we found different viscosities even within the liquid phase of the same sample. To our knowledge, this heterogeneity of the liquid phase has not been reported before for CHCs. It might be due to a miscibility gap, i.e. a phase separation of compounds that occurs only at certain temperatures (Jirát et al., 2009). Miscibility gaps have been reported before from binary systems containing hydrocarbons (Ferloni et al., 1971), rendering it a plausible mechanism for CHC heterogeneity. We cannot rule out that the CHCs on insect body surfaces might form structures different from those on an object slide. To our knowledge, the structural arrangement of CHCs *in situ*, i.e. on insect bodies, has not yet been studied. CHCs are excreted on the cuticle by specialized carrier proteins (lipophorins) (Wang et al., 2021), but there are no reports on enzymes that manipulate structural assembly of CHCs directly on the cuticle so far. Thus, we have little reason to assume that they form any structures beyond the self-assembly that should also happen on artificial surfaces such as object slides.

The picture that emerges from our study is that, at any temperature the insect can experience, CHCs are biphasic, both solid and liquid, but also that the liquid phase is heterogeneous in itself. The phase with lowest viscosity is most abundant, which is why we additionally analysed its behaviour separately here. Its viscosity ranged from 0.05 to 0.6 Pa s in our study, similar to a previous report (0.1 to 0.4 Pa s; Menzel et al., 2019). We suggest regarding this low-viscous phase as a 'matrix' or 'suspending fluid', with more viscous

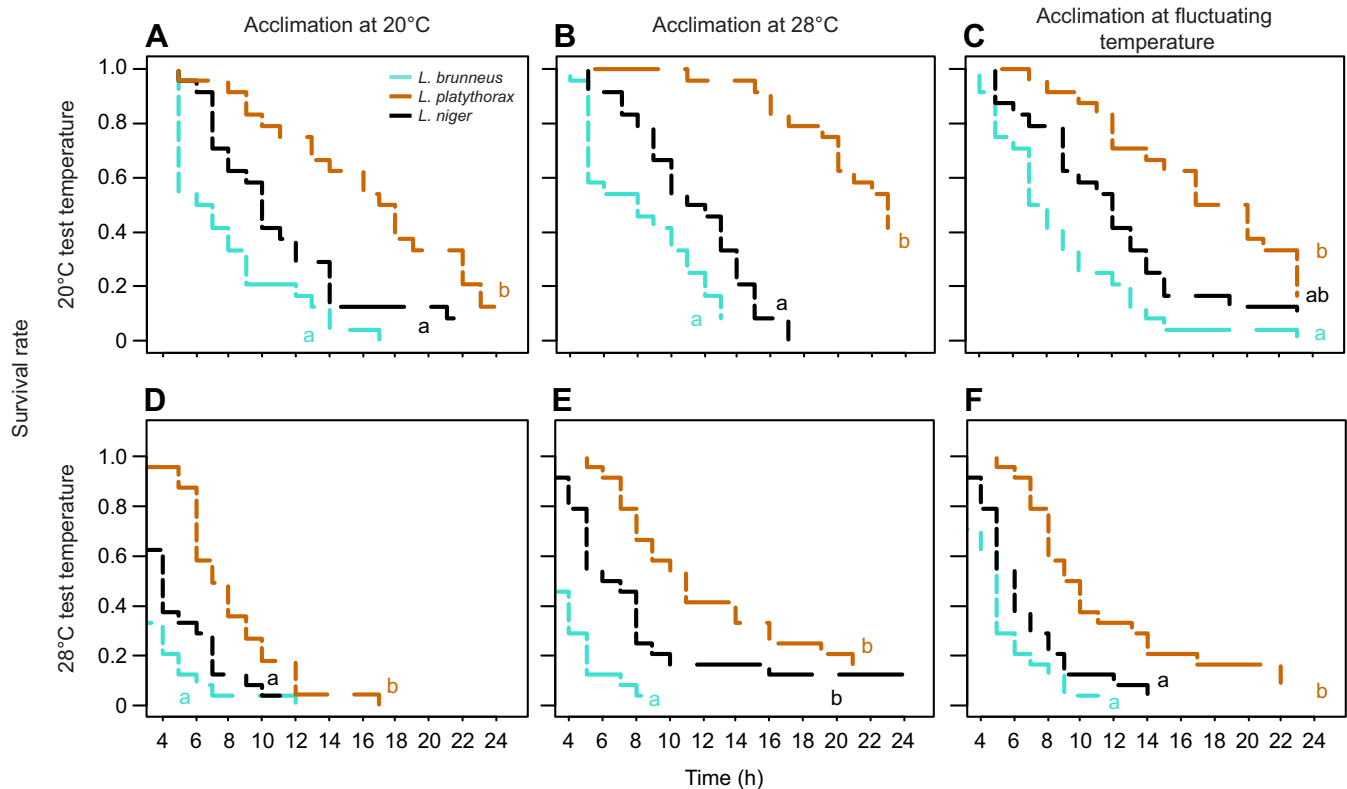


Fig. 8. Drought survival of the three ant species at different temperatures. The plots show survival curves, separately for each test temperature (A–C: 20°C; D–F: 28°C), species and acclimation temperature (20°C, 28°C or fluctuating temperature conditions). Different letters indicate a significant difference according to Cox mixed-effects models.

or solid parts floating in it. Note that the apparent homogeneity of the microrheological CHC samples at 32°C (being entirely liquid with a homogeneous viscosity) might result from the collection procedure before the viscosity measurements, which does not allow the collection of solid or gelified phases. This does not affect any of our conclusions, but especially given the DSC data, it is important to keep in mind that the liquid phase is probably also heterogeneous at higher temperatures.

We hypothesize that heterogeneity of the liquid phase is beneficial for the ant. When temperature drops, certain parts solidify or become more viscous, but there is no risk that the entire layer gelifies simultaneously, which would compromise its functionality all of a sudden. Similarly, a layer that melted completely at a certain temperature would abruptly become more permeable for water, which would be detrimental for the insect as well. Thus, a heterogeneous CHC layer increases the robustness of its physical properties, helping to maintain homeostasis. Hence, CHC composition might experience selection for heterogeneity, at least in habitats with frequent temperature fluctuations. Note that here, heterogeneity refers to the phase behaviour and not necessarily to the more complex chemical composition.

Acclimatory changes in viscosity

In *L. niger* and *L. platythorax*, viscosity of the matrix did not change with acclimation treatment, despite the strong chemical changes. We hypothesize that as a result of phase separation, the CHC changes did not affect matrix viscosity, but rather led to either a higher abundance of more viscous parts, or higher viscosity of these parts. Unfortunately, viscosity cannot be measured for gelified parts, which is why heterogeneity of viscosity is generally hard to quantify if gelified parts are to be included.

Again, *L. brunneus* departs from the other two species, being the only one where the matrix viscosity changed with acclimation. The CHC viscosity of this species was more homogeneous in our analyses, which might limit its ability to acclimate, and indeed did not show acclimatory survival benefits. Viscosity was highest in cool-acclimated workers, and lowest for those from the fluctuating temperature treatment. Here, viscosity and CHC composition can tentatively be linked: in total, the fluctuating temperature treatment (which was least viscous) contained the most fluid compounds (alkenes, alkadienes and methyl-branched alkenes), followed by the 28°C and the 20°C treatment. In turn, the sum of solid to highly viscous CHCs (*n*-alkanes and mono-methyl alkanes) was highest in the 20°C treatment and lowest in the fluctuating temperature treatment (Fig. 3). Assuming a more homogeneous mixture than in the other two species, these effects may explain the observed viscosities.

Melting ranges

Like viscosity, melting ranges of *L. niger* and *L. platythorax* were relatively similar, which is surprising given their strong chemical differences. Given this, it is hard to assign certain melting ranges to chemical compounds. The melting ranges showed much fewer individual peaks than one would expect given the high number of compounds. This indicates that different hydrocarbon molecules interact tightly to form continuous melting ranges rather than a high number of melting peaks (Menzel et al., 2019). This effect should be adaptive because continuous melting makes the CHC layer more robust against temperature fluctuations than sudden melting of larger CHC quantities.

The most prominent acclimation-induced melting peaks (between 30 and 50°C in *L. niger*) are probably caused by *n*-

alkanes and/or terminally branched mono-methyl alkanes. Pure *n*-alkanes of the relevant chain lengths (*n*-C25 to *n*-C33) melt between 54 and 71°C (Lide, 2008). Interestingly though, there was no relevant melting detectable beyond 50°C. Albeit melting detection is affected by the heating rate during DSC, this result suggests that in the CHC mixture, *n*-alkanes melted earlier as a result of hindered packing of the molecules compared with the pure substances. This effect becomes especially pronounced in complex mixtures with many molecules of similar chemical structure (e.g. long hydrocarbon chains with no or only a few branches and kinks). In that case, the molecules mix well, so that areas of ‘pure’ substances can become very small. As a consequence, intermolecular interactions are weaker and melting transitions can occur at lower temperatures. Demixing can occur in liquid phases as a result of diffusion if left for equilibration, but the kinetics are usually much slower than the experimentally applied time frames (as, for example, the time needed for one DSC measurement). This scenario links the two observations that *n*-alkanes were more abundant in warm-acclimated *L. niger* than in the other treatments, but also compared with levels in *L. platythorax*, and that the same is true for melting proportions in the range of 30 to 50°C.

One main new insight from our melting data is that adaptive warm acclimation does not necessarily need more solid compounds – this is shown by the surprisingly few compounds melting between 20 and 28°C. Hence, waterproofing is also possible by the liquid phase if it is viscous enough.

Drought survival

In two of the three ant species, acclimation led to increased drought resistance. This effect was most pronounced at 28°C, but much weaker at 20°C test temperature. While this was expected given that water permeability increases with temperature as a result of CHC melting and increased water vapour pressure, it shows that drought survival should always be measured at multiple temperatures. An earlier study found consistent effects of test temperature on the drought survival of springtails (Chown et al., 2007). Notably, even at 20°C, the 20°C-acclimated workers did not survive better than the 28°C-acclimated ones, which corroborates our assumption that mortality was driven by water loss. It also confirms that acclimatory CHC changes are not only to optimize desiccation resistance – if this was true, ants would always have a ‘warm-acclimated’ profile. Thus, this is evidence that CHC profiles are also constrained by the need to remain fluid to some degree, probably for communication or other purposes (Menzel et al., 2019).

In *L. niger* and *L. platythorax*, warm acclimation and – for *L. platythorax* – also fluctuating acclimation significantly increased survival at 28°C test temperature (Fig. S3). Although *L. brunneus* was the only species with viscosity changes during acclimation, its survival was unaffected by acclimation. However, it is possible (albeit unlikely) that in *L. brunneus*, acclimation and survival might also have been affected by keeping them in smaller worker groups without brood compared with the other two species.

In *L. niger*, the higher survival rates of warm-acclimated workers can be linked to an increase in solid CHCs (*n*-alkanes and possibly mono-methyl alkanes), i.e. those that melted above 28°C (Gibbs and Rajpurohit, 2010). As viscosity is only defined for liquids, this effect did not impact viscosity. Water loss has been linked to acclimation and chemical changes before (Hadley, 1977; Gibbs and Mousseau, 1994; Rajpurohit et al., 2017). However, most studies focused on *n*-alkane abundance or CHC chain length. As shown here, changes in other compounds are similarly important for waterproofing, as exemplified by *L. platythorax*, which showed

clear acclimatory survival benefits but hardly possesses any *n*-alkanes.

Acclimatory strategies

The three ants we studied use different acclimatory strategies, i.e. different approaches to achieve higher waterproofing. *Lasius niger* had the most intuitive strategy: warm-acclimated ants produced more and longer *n*-alkanes, and hence more solid compounds. Indeed, this corresponded to more CHCs melting above 30°C, and a longer survival of warm-acclimated workers. For *L. platythorax*, the picture is less straightforward. Warm acclimation did not result in more (or longer) *n*-alkanes, and there was no increase in CHCs melting above 30°C. We hypothesize that *L. platythorax* acclimates to warmer climates by upregulating CHCs that melt between 10 and 20°C (presumably mono-methyl alkanes). These compounds are liquid above 20°C, but more viscous than the matrix, and hence can reduce water permeability. This strategy seems to be also used by *L. niger*. Warm-acclimated *L. niger* also upregulated mono-methyl alkane production; and the liquid parts of their CHC layers were similarly heterogeneous (Fig. 7B). Unfortunately, the viscosity of highly viscous phases is hard to quantify, as we are approaching the detection limit of Brownian motion. Therefore, a large proportion of the tracer beads in this phase cannot be used to quantify the heterogeneity of the sample. For *L. brunneus*, the acclimatory changes are hardest to explain, as several chemical changes should rather increase than decrease water loss. The CHC profile of this species is more homogeneous, which explains why the viscosity of the matrix changed with acclimation. Here, considering the changes that should enhance drought resistance, warm acclimation seemed to take place mostly by higher overall CHC production and higher average *n*-alkane chain length than by compositional changes in substance classes. However, as for *L. brunneus* acclimation did not result in higher survival, it is unclear whether the observed changes are actually adaptive. The arboreal *L. brunneus* usually nests in the wood or bark of living trees. Thus, the desiccation pressure might be substantially lower than in *L. niger* and *L. platythorax* because even during droughts, its nests should receive some humidity through the tree’s xylem. The lower drought survival of this species might hence be linked to a lower desiccation pressure as a result of its arboreal lifestyle.

Conclusions: CHCs as a functional trait

Functional traits are defined as measurable traits that vary across species and affect the organism’s fitness (McGill et al., 2006). As shown here, CHC profiles can be seen as a functional trait with multiple dimensions. They show strong qualitative differences among species, e.g. concerning their content in unsaturated hydrocarbons. This is related to their ecological niche, because unsaturated compounds are especially common in species from wet habitats (Martin et al., 2008; Van Wilgenburg et al., 2011; Menzel et al., 2017), and CHC changes affect fitness. To understand these fitness affects, we studied here how CHC composition translates to the physical mechanism of waterproofing, and the ants’ ability to enhance drought resistance via acclimation. Although generalizations must be regarded with caution at this stage, it seems possible that profiles rich in methyl-branched alkanes are more heterogeneous, which helps the animals to deal with temperature fluctuations.

Future studies should test how much our results can be generalized across species to better understand the link between CHC composition, acclimation strategy and the ability to acclimate. Here, we need to include further parameters of the CHC profile

relevant for waterproofing. Among others, these include average chain length and *n*-alkane content. Several earlier studies (Gibbs et al., 1991; Gibbs and Mousseau, 1994; Gibbs et al., 1997) showed that they are highly relevant, but they do not tell the entire story, especially in species with only a few *n*-alkanes. Here, multi-species comparisons of physical properties will help us to establish a model on phase behaviour and inter-molecular interactions between different hydrocarbons on the insect cuticle (Krupp et al., 2020; Blomquist and Ginzl, 2021). Further research may then enable us to predict an organism's ability to acclimate and to cope with certain ecological conditions based on its CHC profile.

Acknowledgements

We thank the Obere Naturschutzbehörde (SGD Süd, Thomas Schindwein) and Jürgen Koch (forest district Ober-Olm) for permission to collect ants at the Ober-Olmer Wald (permission no. 42/553-254/287-19). Furthermore, we are grateful to Petra Räder for the DSC measurements.

Competing interests

The authors declare no competing or financial interests.

Author contributions

Conceptualization: B.A., F.M.; Methodology: S.M., B.A., F.M.; Validation: B.A., F.M.; Formal analysis: L.B., S.M., B.A., F.M.; Investigation: L.B., M.W., S.M.; Data curation: L.B., M.W., S.M., B.A.; Writing - original draft: L.B.; Writing - review & editing: B.A., F.M.; Visualization: L.B., F.M.; Supervision: F.M.; Project administration: F.M.

Funding

This study was funded by a Heisenberg fellowship of the Deutsche Forschungsgemeinschaft (DFG) to F.M. (grant no. M.E. 3842/6-1). Furthermore, it was supported by the Deutscher Akademischer Austauschdienst (DAAD, PPP Procope France, project ID: 57388961, to F.M.) with funds from the Bundesministerium für Bildung und Forschung. B.A. was supported by PHC Procope 2018 (project ID: 40427NM) with funds from Ministère de l'Europe et des Affaires étrangères (MEAE) and Ministère de l'Enseignement Supérieur, de la Recherche et de l'Innovation (MESRI).

Data availability

Data are available in Dryad (Menzel et al., 2022): doi:10.5061/dryad.k98sf7m8n.

References

- Abou, B., Gay, C., Laurent, B., Cardoso, O., Voigt, D., Peisker, H. and Gorb, S. (2010). Extensive collection of femtolitre pad secretion droplets in the beetle *Leptinotarsa decemlineata* allows nanolitre microrheology. *J. R. Soc. Interface* **7**, 1745-1752. doi:10.1098/rsif.2010.0075
- Blomquist, G. J. and Bagnères, A.-G. (2010a). Introduction: history and overview of insect hydrocarbons. In *Insect Hydrocarbons: Biology, Biochemistry, and Chemical Ecology* (ed. G. J. Blomquist and A.-G. Bagnères), pp. 3-18. Cambridge University Press.
- Blomquist, G. J. and Bagnères, A.-G. (2010b). Structure and analysis of insect hydrocarbons. In *Insect Hydrocarbons: Biology, Biochemistry, and Chemical Ecology* (ed. G. J. Blomquist and A.-G. Bagnères), pp. 19-34. Cambridge University Press.
- Blomquist, G. J. and Ginzl, M. D. (2021). Chemical ecology, biochemistry, and molecular biology of insect hydrocarbons. *Annu. Rev. Entomol.* **66**, 45-60. doi:10.1146/annurev-ento-031620-071754
- Buellesbach, J., Whyte, B. A., Cash, E., Gibson, J. D., Scheckel, K. J., Sandidge, R. and Tsutsui, N. D. (2018). Desiccation resistance and microclimate adaptation: cuticular hydrocarbon signatures of different Argentine ant supercolonies across California. *J. Chem. Ecol.* **44**, 1101-1114. doi:10.1007/s10886-018-1029-y
- Carlson, D. A., Bernier, U. R. and Sutton, B. D. (1998). Elution patterns from capillary GC for methyl-branched alkanes. *J. Chem. Ecol.* **24**, 1845-1865.
- Chown, S. L., Slabber, S., McGeoch, M. A., Janion, C. and Leinaas, H. P. (2007). Phenotypic plasticity mediates climate change responses among invasive and indigenous arthropods. *Proc. R. Soc. B* **274**, 2531-2537. doi:10.1098/rspb.2007.0772
- Chown, S. L., Sørensen, J. G. and Terblanche, J. S. (2011). Water loss in insects: an environmental change perspective. *J. Insect Physiol.* **57**, 1070-1084. doi:10.1016/j.jinsphys.2011.05.004
- Colinet, H., Sinclair, B. J., Vernon, P. and Renault, D. (2015). Insects in fluctuating thermal environments. *Annu. Rev. Entomol.* **60**, 123-140. doi:10.1146/annurev-ento-010814-021017
- Cooper, R., Lee, H., González, J. M., Butler, J., Vinson, S. B. and Liang, H. (2008). Lubrication and surface properties of roach cuticle. *J. Tribol.* **131**, 014502. doi:10.1115/1.3002327
- De Guzmán, J. (1913). Relación entre la Fluidez y el Calor de Fusión. *An. Soc. Esp. Fis. Quim* **11**, 353-362.
- Drechsler, P. and Federle, W. (2006). Biomechanics of smooth adhesive pads in insects: influence of tarsal secretion on attachment performance. *J. Comp. Physiol.* **192**, 1213-1222. doi:10.1007/s00359-006-0150-5
- Einstein, A. (1905). Über die von der molekularkinetischen Theorie der Wärme geforderte Bewegung von in ruhenden Flüssigkeiten suspendierten Teilchen. *Ann. Phys.* **17**, 549-560. doi:10.1002/andp.19053220806
- Eyring, H. (1935). The activated complex in chemical reactions. *J. Chem. Phys.* **3**, 107-115. doi:10.1063/1.1749604
- Ferloni, P., Geangu-Moisin, A., Franzosini, P. and Rolla, M. (1971). Binary Systems Containing Hydrocarbons IV. Miscibility Gaps in 18 Nitromethane+ 1-, 2-, 3- and 4-alkenes. *Z. Naturforsch. A* **26**, 1713-1716. doi:10.1515/zna-1971-1021
- Ferveur, J.-F. and Cobb, M. (2010). Behavioral and evolutionary roles of cuticular hydrocarbons in Diptera. In *Insect Hydrocarbons: Biology, Biochemistry and Chemical Ecology* (ed. G. J. Blomquist and A.-G. Bagnères), pp. 325-343. Cambridge University Press.
- Gibbs, A. G. (1998). Water-proofing properties of cuticular lipids. *Am. Zool.* **38**, 471-482. doi:10.1093/icb/38.3.471
- Gibbs, A. G. (2002). Lipid melting and cuticular permeability: new insights into an old problem. *J. Insect Physiol.* **48**, 391-400. doi:10.1016/S0022-1910(02)00059-8
- Gibbs, A. and Mousseau, T. A. (1994). Thermal acclimation and genetic variation in cuticular lipids of the lesser migratory grasshopper (*Melanoplus sanguinipes*): effects of lipid composition on biophysical properties. *Physiol. Zool.* **67**, 1523-1543. doi:10.1086/physzool.67.6.30163910
- Gibbs, A. and Pomonis, J. G. (1995). Physical properties of insect cuticular hydrocarbons: The effects of chain length, methyl-branching and unsaturation. *Comp. Biochem. Physiol. B Biochem. Mol. Biol.* **112**, 243-249.
- Gibbs, A. G. and Rajpurohit, S. (2010). Cuticular lipids and water balance. In *Insect Hydrocarbons: Biology, Biochemistry, and Chemical Ecology* (ed. G. J. Blomquist and A.-G. Bagnères), pp. 100-120. Cambridge University Press.
- Gibbs, A., Mousseau, T. A. and Crowe, J. H. (1991). Genetic and acclimatory variation in biophysical properties of insect cuticle lipids. *Proc. Natl. Acad. Sci. USA* **88**, 7257-7260. doi:10.1073/pnas.88.16.7257
- Gibbs, A. G., Chippindale, A. K. and Rose, M. R. (1997). Physiological mechanisms of evolved desiccation resistance in *Drosophila melanogaster*. *J. Exp. Biol.* **200**, 1821-1832. doi:10.1242/jeb.200.12.1821
- Hadley, N. F. (1977). Epicuticular lipids of the desert tenebrionid beetle, *Eleodes armata*: seasonal and acclimatory effects on composition. *Insect Biochem.* **7**, 277-283. doi:10.1016/0020-1790(77)90025-7
- Hartke, J., Sprenger, P. P., Sahm, J., Winterberg, H., Orivel, J., Baur, H., Beuerle, T., Schmitt, T., Feldmeyer, B. and Menzel, F. (2019). Cuticular hydrocarbons as potential mediators of cryptic species divergence in a mutualistic ant association. *Ecol. Evol.* **9**, 9160-9176. doi:10.1002/ece3.5464
- Jiráč, J., Košata, B., Jenkins, A. and McNaught, A. (2009). Compendium of Chemical Terminology – The "Gold Book", 2nd Edition (compiled by A. D. McNaught and A. Wilkinson). IUPAC. Oxford: Blackwell Scientific Publications. IUPAC: Research Triangle Park, NC.
- Kather, R. and Martin, S. J. (2012). Cuticular hydrocarbon profiles as a taxonomic tool: advantages, limitations and technical aspects. *Physiol. Entomol.* **37**, 25-32. doi:10.1111/j.1365-3032.2011.00826.x
- Kather, R. and Martin, S. J. (2015). Evolution of cuticular hydrocarbons in the hymenoptera: a meta-analysis. *J. Chem. Ecol.* **41**, 871-883. doi:10.1007/s10886-015-0631-5
- Kellermann, V., Loeschcke, V., Hoffmann, A. A., Kristensen, T. N., Fløjgaard, C., David, J. R., Svenning, J. C. and Overgaard, J. (2012). Phylogenetic constraints in key functional traits behind species' climate niches: patterns of desiccation and cold resistance across 95 *Drosophila* species. *Evolution* **66**, 3377-3389. doi:10.1111/j.1558-5646.2012.01685.x
- Krupp, J. J., Nayal, K., Wong, A., Millar, J. G. and Levine, J. D. (2020). Desiccation resistance is an adaptive life-history trait dependent upon cuticular hydrocarbons, and influenced by mating status and temperature in *D. melanogaster*. *J. Insect Physiol.* **121**, 103990. doi:10.1016/j.jinsphys.2019.103990
- Leonhardt, S. D., Menzel, F., Nehring, V. and Schmitt, T. (2016). Ecology and evolution of communication in social insects. *Cell* **164**, 1277-1287. doi:10.1016/j.cell.2016.01.035
- Lide, D. R. (2008). *CRC Handbook of Chemistry and Physics*. Boca Raton: CRC.
- Maroncelli, M., Qi, S. P., Strauss, H. L. and Snyder, R. G. (1982). Nonplanar conformers and the phase behavior of solid *n*-alkanes. *J. Am. Chem. Soc.* **104**, 6237-6247. doi:10.1021/ja00387a013
- Martin, S. J., Helanterä, H. and Drijfhout, F. P. (2008). Evolution of species-specific cuticular hydrocarbon patterns in Formica ants. *Biol. J. Linn. Soc.* **95**, 131-140. doi:10.1111/j.1095-8312.2008.01038.x
- McGill, B. J., Enquist, B. J., Weiher, E. and Westoby, M. (2006). Rebuilding community ecology from functional traits. *Trends Ecol. Evol.* **21**, 178-185. doi:10.1016/j.tree.2006.02.002

- Menzel, F., Blaimer, B. B. and Schmitt, T.** (2017). How do cuticular hydrocarbons evolve? Physiological constraints and climatic and biotic selection pressures act on a complex functional trait. *Proc. R. Soc. B* **284**, 20161727. doi:10.1098/rspb.2016.1727
- Menzel, F., Morsbach, S., Martens, J. H., Räder, P., Hadjaje, S., Poizat, M. and Abou, B.** (2019). Communication versus waterproofing: the physics of insect cuticular hydrocarbons. *J. Exp. Biol.* **222**, jeb210807. doi:10.1242/jeb.210807
- Menzel, F., Zumbusch, M. and Feldmeyer, B.** (2018). How ants acclimate: impact of climatic conditions on the cuticular hydrocarbon profile. *Funct. Ecol.* **32**, 657-666. doi:10.1111/1365-2435.13008
- Menzel, F., Baumgart, L., Wittke, M., Abou, B., Lucas, B., Marti, W., Abou, B. and Morsbach, S.** (2022). Data from: Why do ants differ in acclimatory ability? Biophysical mechanisms behind cuticular hydrocarbon acclimation across species. *Dryad Dataset*. doi:10.5061/dryad.k98sf7m8n
- Michelutti, K. B., Soares, E. R. P., Sguarizi-Antonio, D., Piva, R. C., Suárez, Y. R., Cardoso, C. A. L. and Antoniali-Junior, W. F.** (2018). Influence of temperature on survival and cuticular chemical profile of social wasps. *J. Therm. Biol.* **71**, 221-231. doi:10.1016/j.jtherbio.2017.11.019
- Pokorny, T., Lunau, K., Quezada-Euan, J. J. G. and Eltz, T.** (2014). Cuticular hydrocarbons distinguish cryptic sibling species in *Euglossa* orchid bees. *Apidologie* **45**, 276-283. doi:10.1007/s13592-013-0250-5
- Rajpurohit, S., Hanus, R., Vrkoslav, V., Behrman, E. L., Bergland, A. O., Petrov, D., Cvačka, J. and Schmidt, P. S.** (2017). Adaptive dynamics of cuticular hydrocarbons in *Drosophila*. *J. Evol. Biol.* **30**, 66-80. doi:10.1111/jeb.12988
- Seifert, B.** (2008). The ants of Central European tree canopies (Hymenoptera: Formicidae)-an underestimated population? In *Canopy Arthropod Research in Europe* (ed. A. Floren and J. Schmidl), pp. 157-173. Bioform Entomology.
- Spicer, M. E., Stark, A. Y., Adams, B. J., Kneale, R., Kaspari, M. and Yanoviak, S. P.** (2017). Thermal constraints on foraging of tropical canopy ants. *Oecologia* **183**, 1007-1017. doi:10.1007/s00442-017-3825-4
- Sprenger, P. and Menzel, F.** (2020). Cuticular hydrocarbons in ants (Hymenoptera: Formicidae) and other insects: how and why they differ among individuals, colonies, and species. *Myrmecological News*, 30.
- Sprenger, P. P., Burkert, L. H., Abou, B., Federle, W. and Menzel, F.** (2018). Coping with the climate: cuticular hydrocarbon acclimation of ants under constant and fluctuating conditions. *J. Exp. Biol.* **221**, jeb171488. doi:10.1242/jeb.171488
- Steiger, S. and Stöckl, J.** (2014). The role of sexual selection in the evolution of chemical signals in insects. *Insects* **5**, 423-438. doi:10.3390/insects5020423
- Toolson, E. C. and Hadley, N. F.** (1979). Seasonal effects on cuticular permeability and epicuticular lipid composition in *Centruroides sculpturatus* ewing 1928 (Scorpiones: Buthidae). *J. Comp. Physiol.* **129**, 319-325. doi:10.1007/BF00686988
- Van Wilgenburg, E., Symonds, M. and Elgar, M.** (2011). Evolution of cuticular hydrocarbon diversity in ants. *J. Evol. Biol.* **24**, 1188-1198. doi:10.1111/j.1420-9101.2011.02248.x
- Wang, Y., Ferveur, J. F. and Moussian, B.** (2021). Eco-genetics of desiccation resistance in *Drosophila*. *Biol. Rev.* **96**, 1421-1440. doi:10.1111/brv.12709
- Wittke, M., Baumgart, L. and Menzel, F.** (2022). Cuticular hydrocarbons in insects: interference of communication and waterproofing in a multifunctional trait. *Funct. Ecol.* doi:10.1111/1365-2435.14104

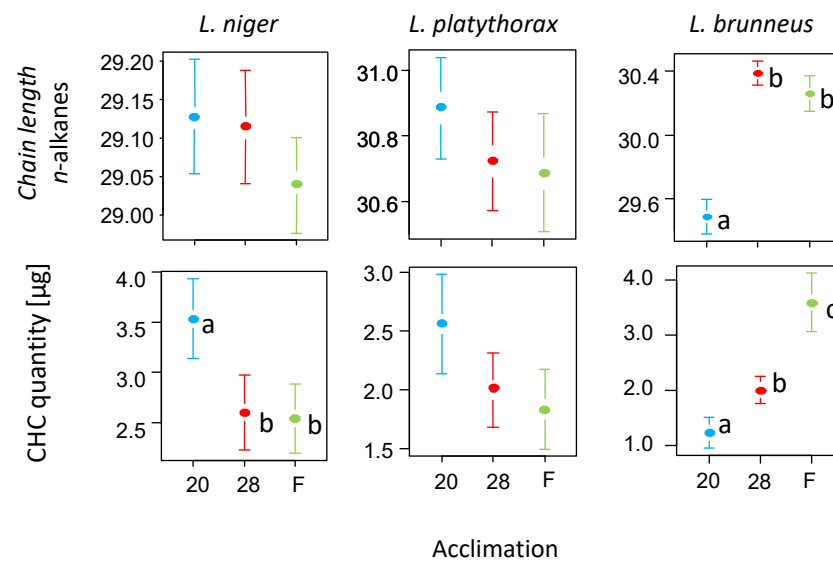


Fig. S1. Acclimatory differences of further CHC traits. Average chain length of *n*-alkanes, and absolute CHC quantity in µg. The graphs show means and standard errors for the three acclimation treatments (20°C: blue; 28°C: red; fluctuating: green). Plots with same letters (or without letters) are not significantly different according to linear mixed-effects models.

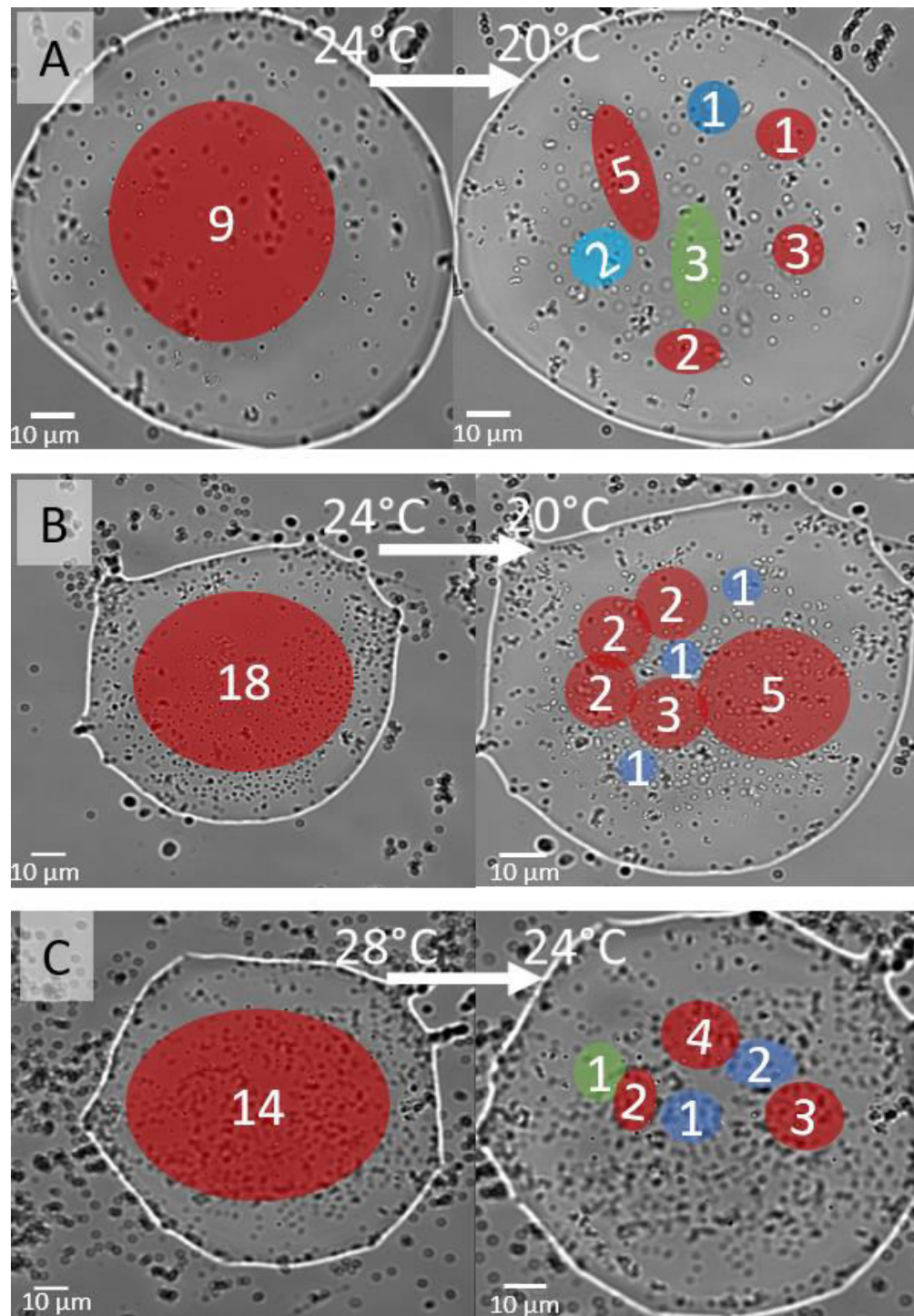


Fig. S2. Transition from homogeneous to heterogeneous phase behaviour during cooling in cuticular hydrocarbon drops with melamine beads (magnification 100x), in (A, B) *L. platythorax* and (C) *L. brunneus*. Coloured areas indicate fields with the same viscosity (red lowest and blue highest) with the number of beads measured in the field.

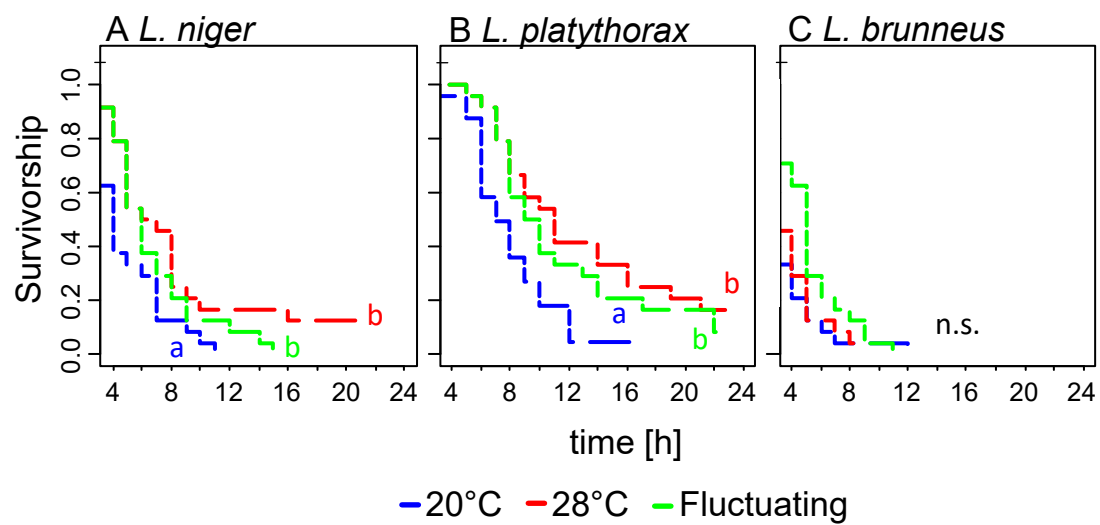


Fig. S3. Survival of (A) *Lasius niger*, (B) *L. platythorax* and (C) *L. brunneus* workers from the three acclimation treatments, only at test temperature 28 °C. Significance of differences (as indicated by letters) was calculated using separate Cox-mixed effects models for each species.

Table S1. Cuticular hydrocarbon profile of *L. niger*. The table shows retention index and mean abundance (\pm standard error) for each hydrocarbon. See also Wittke et al. (2022).

	retention index	abundance (%)
<i>n</i> -C25	25.01	0.26 \pm 0.05
<i>n</i> -C26	26	0.13 \pm 0.02
<i>n</i> -C27	27	2.44 \pm 0.34
5,11-;5,13-DiMeC27	27.81	0.14 \pm 0.02
<i>n</i> -C28	28	0.39 \pm 0.04
4-;2-MeC28	28.61	0.28 \pm 0.03
C29-alkene	28.8	0.31 \pm 0.06
<i>n</i> -C29	28.97	3.08 \pm 0.31
13-;15-MeC29	29.27	1.53 \pm 0.07
5-MeC29	29.49	2 \pm 0.17
11,15-DiMeC29	29.56	0.4 \pm 0.04
9,15-DiMeC29	29.65	3.83 \pm 0.24
3-MeC29	29.73	0.56 \pm 0.08
5,15-DiMeC29	29.77	2.88 \pm 0.14
7,11,15-TriMeC29	29.92	1.16 \pm 0.1
<i>n</i> -C30	29.98	0.51 \pm 0.06
5,9,13-TriMeC29	30.04	0.9 \pm 0.07
12-;13-;14-;15-MeC30; cf. 3,7,15-TriMeC29	30.32	1.13 \pm 0.04
2-;4-MeC30	30.56	2.17 \pm 0.1
C31-ene 1	30.77	1.67 \pm 0.13
C31-ene 2	30.85	0.44 \pm 0.03
<i>n</i> -C31	30.97	2.21 \pm 0.15
Unknown; RI = 31.13	31.13	0.48 \pm 0.1
9-;11-;13-;15-MeC31	31.32	9.95 \pm 0.29
cf. 5-MeC31	31.54	1.34 \pm 0.17
9,23-DiMeC31	31.69	17.59 \pm 0.51
5,x-DiMeC31 (x=13;15)	31.84	6.51 \pm 0.32
7,x,y-TriMeC31 (x=11,y=15?)	31.92	1.97 \pm 0.13
3,9-;3,11-DiMeC31	32.02	3.46 \pm 0.09
cf. 11-;12-;13-;14-;15-;16-MeC32	32.29	2.15 \pm 0.07
10,14-;x.16-DiMeC32	32.58	2.46 \pm 0.08
C33-alkene	32.75	0.96 \pm 0.07
6,14-;6,16-DiMeC32; 3-MonoMeC32	32.85	0.37 \pm 0.05
Unknown; RI = 33.04	33.04	0.52 \pm 0.04
Unknown; RI = 33.17	33.17	0.27 \pm 0.03
9-;11-;13-;15-MeC33	33.3	3.55 \pm 0.14
11,15-DiMeC33	33.62	1.27 \pm 0.15
9,x-DiMeC33 (cf. x=15)	33.7	7.36 \pm 0.3
5,15-;5,17-DiMeC33	33.83	2.06 \pm 0.16
7,x,y-TriMeC33	33.98	0.81 \pm 0.06
3,9-;3,11-DiMeC33	34.1	1.84 \pm 0.11
cf. C34 MonoMe	34.33	0.61 \pm 0.05
unknown; RI = 34.61	34.61	0.75 \pm 0.06
11-;13-;15-;17-MeC35	35.33	0.54 \pm 0.04
cf. 11,23-DiMeC35	35.64	2.39 \pm 0.12

x,y-DiMeC35	35.76	0.68 ± 0.09
Unknown; RI = 35.95	35.95	0.22 ± 0.03
Unknown; RI = 36.08	36.08	0.17 ± 0.03
Unknown; RI = 36.28	36.28	0.16 ± 0.02
Unknown; RI = 36.6	36.6	0.21 ± 0.03
Unknown; RI = 37.27	37.27	0.12 ± 0.02
<u>cf. 11,23-DiMeC37</u>	<u>37.6</u>	<u>0.81 ± 0.09</u>

Table S2. Cuticular hydrocarbon profile of *L. platythorax*. The table shows retention index and mean abundance (\pm standard error) for each hydrocarbon. See also Wittke et al.(2022)

	retention index	abundance (%)
<i>n</i> -C27	27.05	0.17 \pm 0.03
<i>n</i> -C28	28.01	0.23 \pm 0.05
<i>n</i> -C29	29.02	0.55 \pm 0.08
<i>n</i> -C30	30.02	0.39 \pm 0.1
<i>n</i> -C31	31.02	0.52 \pm 0.09
7-MeC31	31.44	0.02 \pm 0
13,17-DiMeC31	31.57	0.03 \pm 0.01
7,x-DiMeC31	31.67	0.27 \pm 0.04
5,x-DiMeC31	31.83	0.01 \pm 0
<i>n</i> -C32	32.03	0.2 \pm 0.04
5,9,15-TriMeC31	32.1	0.07 \pm 0.01
cf 10-;11-;12-;13-MeC32	32.33	0.17 \pm 0.02
8,x-DiMeC32	32.63	0.32 \pm 0.05
6,x-DiMeC32	32.76	0.06 \pm 0.01
8,12,16-TriMeC32	32.93	0.04 \pm 0.01
<i>n</i> -C33	33.01	0.52 \pm 0.05
17-;15-;13-;11-;9-;7-MonoMeC33	33.37	3.51 \pm 0.18
cf 11,15-;13,17-DiMeC33	33.56	2.07 \pm 0.12
9,x-;11,x-;13,x-DiMeC33	33.65	3.83 \pm 0.25
7,17-;7,19-;7,21-DiMeC33	33.7	3.66 \pm 0.18
5,9-;5,15-DiMeC33	33.81	3.96 \pm 0.2
7,17,21-TriMeC33	33.94	4.51 \pm 0.34
5,9,17-TriMeC33	34.08	3.6 \pm 0.14
11-;12-;13-;14-;15-;16-;17-MeC34	34.33	1.59 \pm 0.06
unknown TriMeC34	34.59	3.04 \pm 0.08
8,12,16-TriMeC34	34.95	1.2 \pm 0.07
4,8,x-TriMeC34	35.18	0.1 \pm 0.01
13-;15-;17-MonoMeC35	35.31	5.77 \pm 0.18
13,21-;11,x-DiMeC35	35.33	14.46 \pm 0.71
7,19-;7,21-DiMeC35	35.71	7.29 \pm 0.34
cf 11,x,23-TriMe35	35.8	4.66 \pm 0.28
7,x,y-TriMeC35	35.95	5.45 \pm 0.38
3,11-DiMeC35	36.09	3.45 \pm 0.11
10-;11-;12-;13-;14-;15-;16-;17-;18-MeC36	36.32	1.41 \pm 0.06
unknown TriMeC36	36.58	1.97 \pm 0.06
8,12,22-TriMeC36	36.96	0.74 \pm 0.06
13-;15-;17-MeC37	37.3	2.21 \pm 0.14
9,x-;11,x-;13,x-;15,x-DiMe37	37.6	5.73 \pm 0.3
7,23-;7,25-DiMeC37	37.69	2.81 \pm 0.12
7,17,25-;7,19,23-;9x,y-TriMeC37)	37.98	4.93 \pm 0.14
3,11-DiMeC37 and (much less) 5,9,15-TriMeC37	38.07	1.36 \pm 0.08

cf. internally branched MonoMeC39	39.33	0.44 ± 0.05
7,x-;11,x-;13,x-;15,x-DiMeC39	39.58	1.55 ± 0.16
5,27-DiMeC39 (tentatively)	39.78	0.25 ± 0.04
7,x,y-TriMeC39	39.92	0.54 ± 0.05
cf 11,x-DiMeC41	NA	0.13 ± 0.02
cf 7,x-DiMeC41	NA	0.22 ± 0.05

Table S3. Cuticular hydrocarbon profile of *L. brunneus*. The table shows retention index and mean abundance (\pm standard error) for each hydrocarbon.

	retention index	abundance (%)
<i>n</i> -C23	22.97	0.11 \pm 0.02
<i>n</i> -C24	23.97	0.1 \pm 0.02
<i>n</i> -C25	24.98	0.17 \pm 0.03
cf <i>n</i> -C26	25.99	0.23 \pm 0.03
<i>n</i> -C27	27	0.74 \pm 0.09
cf 4-MeC27	27.72	0.12 \pm 0.03
<i>n</i> -C28	27.99	0.67 \pm 0.07
<i>n</i> -C29	29	2.33 \pm 0.2
11-,13-MeC29	29.31	0.04 \pm 0.01
9-MeC29	29.36	0.15 \pm 0.02
3-MeC29	29.75	0.65 \pm 0.08
<i>n</i> -C30	30.01	0.97 \pm 0.09
C31-ene	30.67	1.14 \pm 0.06
C31-ene	30.84	0.59 \pm 0.06
<i>n</i> -C31	31.01	3.19 \pm 0.26
11-MeC31	31.34	2.71 \pm 0.17
9-MeC31	31.38	0.37 \pm 0.13
7-MeC31	31.43	1.8 \pm 0.11
5-MeC31	31.53	0.59 \pm 0.02
11,15-DiMeC31	31.59	0.57 \pm 0.02
11,x-,9,x-DiMeC31 and C32-ene	31.69	1.11 \pm 0.04
3-MeC31 and 5,x-DiMeC31	31.77	2.32 \pm 0.13
<i>n</i> -C32	32.03	0.75 \pm 0.05
unknown internally branched monomethyl alkane (C32)	32.33	0.12 \pm 0.02
C33-diene	32.55	13.96 \pm 0.43
C33-ene	32.71	11.98 \pm 0.24
C33-ene	32.88	3.08 \pm 0.2
<i>n</i> -C33	33.05	1.67 \pm 0.13
unknown C33-methyl-branched alkene	33.1	0.83 \pm 0.06
unknown methyl-branched alkene (C33)	33.2	0.35 \pm 0.03
11-,13-,15-,17-MeC33	33.34	3.86 \pm 0.17
9-MeC33	33.4	0.56 \pm 0.08
7-MeC33	33.45	3.38 \pm 0.14
5-MeC33	33.55	2.09 \pm 0.06
unknown	33.59	0.26 \pm 0.05
11,23-DiMeC33	33.69	2.58 \pm 0.09
5,x-DiMeC33	33.82	1.48 \pm 0.06
unknown	34.05	0.45 \pm 0.04
unknown	34.35	0.21 \pm 0.04
unknown	34.48	0.14 \pm 0.04
C35-diene	34.58	16.24 \pm 0.42
C35-ene	34.73	6.89 \pm 0.19
C35-ene	34.92	0.7 \pm 0.07
C35-diene	35.07	0.57 \pm 0.06
C35-methyl-branched alkene	35.11	0.95 \pm 0.09

unknown	35.22	0.13 ± 0.02
13-;15-;17-MeC35	35.34	1.18 ± 0.07
7-MeC35	35.48	0.43 ± 0.05
unknown unsaturated	35.65	0.48 ± 0.06
unknown unsaturated	35.72	0.29 ± 0.04
5,x-DiMeC35	35.83	0.3 ± 0.04
unknown saturated	36.07	0.1 ± 0.02
C37-diene	36.4	0.14 ± 0.04
unknown	36.46	0.15 ± 0.04
C37-diene	36.61	1.71 ± 0.13
C37-ene and C37-diene	36.73	0.69 ± 0.06
C37-ene	36.74	0.23 ± 0.07
C37-diene	36.82	0.22 ± 0.03
unknown unsaturated	37.09	0.13 ± 0.03
unknown	37.34	0.09 ± 0.02

Table S4. Statistical results on the CHC analysis. The table shows results of linear mixed-effects models, with acclimation regime and fragment type (except for *L. brunneus*) as fixed factors (interactions allowed) and colony and observer (colony only for *L. brunneus*) as random effects. The dependent variables were transformed if necessary to obtain normally distributed model residuals (see table).

class	variable	Chi ²	df	p	transformation used
<i>L. niger</i>					
n-alkanes	acclimation	56.59	2	<0.0001	arcsin-sqrt
	fragment	0.01	1	0.91	
	acclimation x fragment	1.10	2	0.58	
monomethyl	acclimation	156.80	2	<0.0001	none
	fragment	0.04	1	0.85	
	acclimation x fragment	0.062	2	0.73	
dimethyl alkanes	acclimation	97.60	2	<0.0001	none
	fragment	0.66	1	0.42	
	acclimation x fragment	0.03	2	0.84	
trimethyl alkanes	acclimation	3.91	2	0.14	arcsin-sqrt
	fragment ²	15.54	1	<0.0001	
	acclimation x fragment	2.06	2	0.36	
alkenes	acclimation	22.80	2	<0.0001	none
	fragment	0.65	1	0.42	
	acclimation x fragment	1.59	2	0.45	
<i>L. platythorax</i>					
n-alkanes	acclimation	15.60	2	0.0004	sqrt
	fragment ¹	27.56	1	<0.0001	
	acclimation x fragment	3.53	2	0.17	
monomethyl ³	acclimation	228.06	2	<0.0001	none
	fragment	1.01	1	0.32	
	acclimation x fragment	0.06	2	0.97	
dimethyl alkanes ³	acclimation	1.60	2	0.45	sqrt
	fragment	2.26	1	0.13	
	acclimation x fragment	0.76	2	0.68	
trimethyl alkanes	acclimation	174.71	2	<0.0001	none
	fragment ²	37.85	1	<0.0001	
	acclimation x fragment	2.54	2	0.28	
<i>L. brunneus</i>					
n-alkanes	acclimation	35.41	2	<0.0001	arcsin-sqrt
monomethyl	acclimation	29.37	2	<0.0001	sqrt
dimethyl alkanes	acclimation	1.48	2	0.48	log
alkenes	acclimation	60.42	2	<0.0001	arcsin-sqrt
methyl alkenes	acclimation	65.13	2	<0.0001	arcsin-sqrt
alkadienes	acclimation	22.65	2	<0.0001	arcsin-sqrt

¹more *n*-alkanes in small fragments; ²less trimethyl alkanes in small fragments; ³according to Shapiro-Wilks test, model residuals deviated from normal distribution, but histograms showed a near-normal distribution. For these two cases, we performed a permutational ANOVA (command *adonis*, package *vegan*) with the same parameters as in the linear mixed-effects models, and obtained similar results. Therefore, we report linear mixed-model results above also for these cases.

Table S5. PERMANOVA results on the effects of fluctuation per se, temperature treatment, and colony on CHC variation. To test whether fluctuating conditions differed systematically from constant ones, we created two variables, ‘const/fluct’ (constant vs. fluctuating conditions) and ‘temperature’ (nested in const/fluct, with the two factor levels 20 °C and 28°C). Interactions between colony and both factors are included in the model. The table shows df, pseudo-F, R² and p values.

		df	pseudo-F	R ²	p
<i>Lasius niger</i>	const/fluct	1	0.8	0.003	0.48
	colony	11	8.3	0.32	0.001
	temperature	1	65.6	0.23	0.001
	colony x const/fluct	11	1.0	0.039	0.42
	temperature x colony	11	1.0	0.039	0.37
<i>Lasius platythorax</i>	const/fluct	1	1.3	0.003	0.28
	colony	11	21.4	0.50	0.001
	temperature	1	98.9	0.21	0.001
	colony x const/fluct	11	1.3	0.031	0.16
	temperature x colony	11	1.2	0.027	0.22
<i>Lasius brunneus</i>	const/fluct	1	23.3	0.16	0.001
	colony	10	4.0	0.27	0.001
	temperature	1	18.6	0.13	0.001
	colony x const/fluct	8	1.6	0.086	0.068
	temperature x colony	6	2.3	0.094	0.008

Table S6. Statistical results on the survival assays. The table shows results of Cox mixed-effects models, with df, χ^2 and p values. Firstly, we constructed a comprehensive model with all test temperatures, species, and acclimation treatments. To further understand specific effects, we then created two models specific to a test temperature (20 °C and 28 °C). Then, acclimatory effects were tested in separate models for each combination of test temperature and species. Finally, to compare survival effects across species, we created acclimation treatment-specific models. Since the time of death was uncertain for some ants, we conducted two parallel analysis, treating them as if they had died a) in the first hour of the experiment or b) directly before the first observation.

Dataset	Fixed effect	Df	Unknown deaths treated as death in the first hour		Unknown deaths treated as death directly before observation	
			χ^2	p	χ^2	P
Comprehensive	Acclimation	2	28.15	<0.001	32.67	<0.001
	Species	2	39.08	<0.001	37.80	<0.001
	Test temperature	1	131.53	<0.001	170.72	<0.001
	Acclimation x species	4	16.33	0.003	17.37	0.002
	Acclimation x test temperature	2	8.49	0.014	13.16	0.001
Specific to test temperature 20 °C	Acclimation	2	5.05	0.080	4.69	0.096
	Species	2	50.07	<0.001	51.65	<0.001
	Acclimation x species	4	7.03	0.134	6.96	0.138
Specific to test temperature 28 °C	Acclimation	2	27.61	<0.001	27.44	<0.001
	Species	2	26.10	<0.001	26.57	<0.001
	Acclimation x species	4	12.50	0.014	12.84	0.002
Specific to test temperature and species						
<i>L. niger</i> 20 °C	Acclimation	2	1.98	0.371	1.98	0.371
<i>L. niger</i> 28 °C	Acclimation	2	17.00	<0.001	17.16	<0.001
<i>L. platythorax</i> 20°C	Acclimation	2	9.28	0.010	9.28	0.010
<i>L. platythorax</i> 28 °C	Acclimation	2	18.89	<0.001	18.89	<0.001
<i>L. brunneus</i> 20 °C	Acclimation	2	1.00	0.605	0.77	0.679
<i>L. brunneus</i> 28 °C	Acclimation	2	4.16	0.125	3.95	0.139
Specific to acclimation treatment						
20 °C acclimation	Test temperature	1	63.69	<0.001	97.45	<0.001
	Species	2	25.58	<0.001	27.59	<0.001
	Test temperature x species	2	1.84	0.400	0.19	0.908
28 °C acclimation	Test temperature	1	24.95	<0.001	39.72	<0.001
	Species	2	38.98	<0.001	40.50	<0.001
	Test temperature x species	2	5.31	0.070	11.02	0.004
Fluctuating acclimation	Test temperature	1	44.88	<0.001	52.82	<0.001
	Species	2	23.70	<0.001	24.03	<0.001
	Test temperature x species	2	0.65	0.72	1.02	0.599